



Antimicrobial and antifouling surfaces through polydopamine bio-inspired coating

Yi-Wen Zhu, Yu-Jie Sun, Ju-Lin Wang* , Bing-Ran Yu* 

Received: 27 July 2021 / Revised: 23 August 2021 / Accepted: 31 August 2021 / Published online: 2 November 2021
© Youke Publishing Co., Ltd. 2021

Abstract The increasing antibiotic treatment failure is attributed to the increasing emergence of drug-resistant bacteria, and the attachment of these bacteria to the surface of implantation materials often leads to dangerous bacterial biofilm formation on the implant surface. Thus, this creates an urgent need to develop new antibacterial material and antifouling implants. Polydopamine (PDA), as a mussel-inspired material, has many advantageous properties, such as a simple preparation procedure, excellent hydrophilicity and biocompatibility, strong adhesive performance, easy functionalization, outstanding photothermal conversion effect, and strong quenching effect. PDA has increasingly attracted much interest not only for its adherence to

virtually all types of surfaces but also as it provides a simple and versatile approach to functionalize material surfaces to obtain a variety of multifunctional nanomaterials. In this review, we mainly focus on the preparation and polymerization mechanism of PDA systems and then provide a compilation of several reports on the PDA surface modification of various nanomaterials and material surfaces, including metals, metal oxides, carbons, and polymers. Finally, we summarize the advantages and disadvantages of polydopamine surface-modified nanomaterials.

Keywords Polydopamine (PDA); Adhesion; Modification; Antibacterial; Antifouling

Yi-Wen Zhu and Yu-Jie Sun have contributed equally to this work.

Y.-W. Zhu, Y.-J. Sun, B.-R. Yu*
State Key Laboratory of Chemical Resource Engineering,
Beijing University of Chemical Technology, Beijing 100029,
China
e-mail: yubr@mail.buct.edu.cn

Y.-W. Zhu, Y.-J. Sun, B.-R. Yu
Key Laboratory of Biomedical Materials of Natural
Macromolecules, Ministry of Education, Beijing University of
Chemical Technology, Beijing 100029, China

Y.-W. Zhu, Y.-J. Sun, B.-R. Yu
Laboratory of Biomedical Materials, College of Materials
Science and Engineering, Beijing University of Chemical
Technology, Beijing 100029, China

J.-L. Wang*
Laboratory of Electrochemical Process and Technology for
Materials, College of Materials Science and Engineering,
Beijing University of Chemical Technology, Beijing 100029,
China
e-mail: Julinwang@126.com

1 Introduction

The development of drug-resistant bacterial strains makes traditional antibiotics become less efficient [1]. The increasing emergence of drug-resistant bacteria not only caused the failure of antibiotic treatment but also aggravated the economic burden of the patients due to the prolonged hospitalizations [2]. It is of great urgency to develop new and potent antibacterial materials. Besides, the numbers of both joint replacements and dental implantations are increasing recently; therefore, it is of great urgency to combat implant-associated infection [3].

In recent years, mussel-inspired materials attract considerable research attention, because they adhere to virtually all types of surfaces, even if the surface is wet. Polydopamine (PDA), as a mussel-inspired material, has many properties, such as a simple preparation procedure, excellent biocompatibility hydrophilicity and biocompatibility [4], strong adhesive property, easy functionalization,



outstanding photothermal conversion effect, and strong quenching effect. Various substrates, such as ceramics, noble metals, metal oxides, semiconductors, silica, mica, and even some synthetic polymers, have been surface-functionalized with PDA [5]. PDA has increasingly attracted considerable interest not only for its adherence to virtually all types of surfaces but also as it provides a simple and versatile approach to functionalize material surfaces to obtain a variety of multifunctional nanomaterials. Owing to its excellent biocompatibility, biodegradability, and photoconversion efficiency, PDA has been recently used to functionalize nanomaterials for antibacterial studies [6].

The attachment of bacteria to the material surface often poses potential risks, such as leading to dangerous bacterial biofilm accumulation on the implant surface [7]. PDA can be used as a surface modification material to obtain PDA-modified surfaces, onto which antibacterial materials can be applied. Here, we compile numerous studies on the surface modification by PDA of various organic and inorganic nanomaterials, including metals, metal oxides, carbons, and polymers. The advantages of PDA coatings are: (1) strong interaction between polymer layers and substrate with excellent long-term stability in most environments [8]; (2) simultaneously serving as reductant, introducing a diversity of metallic nanoparticles (NPs) onto various substrates via reduction of the metal ions, without the need for additional reduction [9]; (3) mild reaction conditions and nondestructive to substrates; and (4) offering numerous reactive groups, like catechol and amino groups, which can be used as a robust platform for further functionalization [10].

Since the pioneering study by Lee et al. [11] in 2007, many PDA surface-modified materials have been reported. For instance, several bio-inspired catechol and their derivatives for surface modification, as well as the design, synthesis, adsorption mechanism, stability, and applications of PDA were reviewed by Ye et al. in 2011 [12]. Later, in 2014, Liu et al. [13] discussed the preparation of PDA and derivatives together with their application prospects in environmental, energy, and biomedical fields. Also, Lynge et al. [14] summarized biomedical applications on the basis of surface modification by PDA coating. In addition, in 2017, Batul et al. [15] reviewed the research progress on the application of PDA in the biomedical field and discussed the polymerization mechanisms. Given the biocompatibility and functionality of PDA, as well as its morphological versatility, PDA coating plays an irreplaceable role in biological applications, such as in antimicrobials for infection prevention. Chen et al. [16] analyzed and verified that PDA is composed mainly of almost flat oligomers, stacking through π - π interactions and forming aggregates similar to graphite. Additionally,

the main components of PDA are small oligomers rather than large polymers. Mrówczyński et al. [17] found that PDA may form by means of oligomers (probably mixtures up to octamers) instead of high molecular weight polymers, and hydrogen bonds and π -stacking form supramolecular structure of oligomers. Using a one-step method, Batul et al. [18] loaded PDA NPs with gentamicin in situ through a polymerization process, and the resulting NPs had high drug loading efficiency and retained their antimicrobial activity. Similarly, Wu et al. [19], Ran et al. [20], Ma et al. [21], and other researchers independently modified PDA NPs with various antibiotic compounds, which were effective in inhibiting or killing bacteria. In the study of Shang et al. [22], a hollow PDA shell was obtained by coating it on monodisperse sulfated polystyrene (SPS) and subsequently removing it with trichloromethane. Wang et al. [23] creatively used the bio-inspired melanin solid NPs and hollow NPs as ultraviolet light absorber in order to enhance the shielding properties of polymers. Meanwhile, Li et al. [24] designed and prepared hybrid ZnO/PDA/arginine-glycine-aspartic acid-cysteine (RGDC) nanorod (NR) arrays to not only enhance the osteoinductivity, but also effectively kill bacteria simultaneously.

The PDA research on the modification of different materials has been developing rapidly, and the aim of this review is to summarize recent significant advancements in PDA research. First, we describe the preparation and polymerization mechanism of PDA systems. After that, we compile many studies on the surface modification of various nanomaterials and material surfaces by PDA, including metals, metal oxides, carbons, and polymers. Finally, we summarize and explain related biomedical applications [25].

2 Mechanisms and properties of PDA

2.1 Adhesion capability and mechanism

Mussel is the common name for members of various bivalve mollusk families, which live on coastal regions, in the intertidal zone, attached by their strong byssal threads. Several research studies have shown that the byssal thread is rich in *Mytilus edulis* foot protein [26], whose essential components Levodopa (L-DOPA) and lysine amino acids play crucial roles in the strong adhesion of mussels [27]. As a derivative of L-DOPA, dopamine (DA), a neurotransmitter commonly used in clinical treatment of Parkinson's disease and other diseases, possesses the catechol structure of L-DOPA and amino functional groups of amino acid, which combines critical factors necessary for strong adhesive function. In fact, under oxidation conditions, catechins and their derivatives can aggregate

spontaneously and form polymer coating that sticks tightly to solid material surfaces.

2.2 Polymerization mechanism and properties of PDA

Under oxygen-containing conditions, dopamine (DA) monomers self-polymerize in an aqueous solution to form an oligomer, and high molecular weight polymer can be obtained through a cross-linking reaction, ultimately producing the supramolecular aggregates of PDA under the effect of the covalent and non-covalent interactions in the reaction system. Although the polymerization mechanism and molecular structure of PDA remain unclear, the following speculations about this process have been put forward by some researchers. First, DA quinone is generated by intramolecular cyclization reaction of DA via 1,4-Michael addition. Then, oxidation and rearrangement turn DA quinone into an indole structure, namely 5,6-dihydroxyindole, whose further oxidation product, 5,6-indolequinone, undergoes a polymerization reaction to form dimers and other oligomers. These oligomers are further polymerized to produce PDA through an anti-disproportionation reaction with catechol and o-quinone [10, 28]. The oxidation route is so complicated that it leads to the highly versatile structure of PDA and insolubility in most solvents, except for strong alkaline solutions.

2.3 PDA surface deposition method

In a humid atmosphere, DA shows strong adhesion to both organic and inorganic surfaces. This is attributed to the formation of strong but reversible coordinate bonds with inorganic materials, and covalent bonds with organic substrates [26]. Inspired by mussel bionics, Lee et al. [29] found that the catecholamine derivative of DA, and its polymer, PDA, can stick to almost all solid substrates. When acting on diverse materials, adhesion mechanism is mediated by various interactions, including hydrogen bonding, chelation, static electricity, and hydrophobic interaction [30]. Metal–oxygen coordination bonds can be formed between catechol and metal/metal oxide/metal sulfide surfaces, which provide strength as strong as covalent bonds [31]. Furthermore, the binding between catechol and metal oxide is pH dependent, that is, hydrogen bonds are mainly formed in acidic environment, while metal–oxygen coordination bonds at neutral to basic pH [31]. Functional PDA coatings are also used on organic materials. This is due to the formation of connective covalent bonds between the two components if nucleophilic groups that can react with o-quinone previously oxidized by catechol groups through Michael-type addition or Schiff base reaction, such as sulfhydryl, amino, and

imino, are present on solid surfaces [32]. In general, regarding polar polymer, linking phenolic hydroxyl groups to surfaces by hydrogen bonds, or even covalent bond, results in the primary adhesion, while hydrophobic or π – π interactions have a crucial part when catechol contacts non-polar polymers. For hydrophobic substrates, the direct effect of the PDA-based modification is achieving hydrophilization. Polyethylene (PE), polyvinylidene fluoride (PVDF), and polytetrafluoroethylene (PTFE) were coated with PDA, and the water contact angle measurement indicated obvious improvement in hydrophilicity of these three polyolefin porous membranes [32]. The surface morphology and sedimentary dynamic of PDA can be controlled by the concentration, solution pH, and reaction time. Some recent research found that DA at a low concentration ($< 0.5 \text{ mg}\cdot\text{ml}^{-1}$) could effectively reduce the formation of particles by self-polymerization and aggregation between particles which was prone to increase the coating roughness [33]. Similarly, reducing the immersion time of the substrate can adjust the coating thickness. In general, for the purpose of modifying solid substrates, Tris buffer (pH 8.5) and 5–6-h reaction time are usually used for research [34].

2.4 Photothermal conversion effect of PDA-coated substrates

PDA coating can be easily formed on various kinds of substrates and has an outstanding biocompatibility and hardly any immune response. In addition, due to its ability of converting near-infrared radiation to thermal energy, PDA is expected to be used as a photothermal material in the treatment of tumors and other diseases, as well as a bactericidal. In recent years, researchers have taken more interest in photothermal therapy as a powerful tool against bacterial infection [33, 34]. Compared with chemotherapy, photothermal therapy (such as polypyrrole (PPy) and PDA) has an excellent broad-spectrum bacterial effect by producing heat [35]. Although near-infrared (NIR) radiation itself is almost not toxic to most organisms, immense heat is produced locally by photothermal agents. For most pathogens, a partial increase in the temperature will induce bacterial protein denaturation and ultimately bacterial cell death. This method takes just a few minutes of irradiation and has no risk of drug resistance development. Based on the above-mentioned advantages, numerous functional materials, such as PDA, have been used as photothermal agents. PDA, as a promising coating platform for medical devices, combines multiple useful functions, which have been applied to fight against bacterial infection by synergistic effects. Undoubtedly, a system that consists of two or more kinds of antibacterial strategies will have a better effect compared with single approach.

PDA, as a mussel-inspired polymer, can be obtained from DA. It exhibits many desirable properties which attract the attention of researchers. The excellent performances of PDA were utilized adequately in biological materials, especially in antibacterial field. As shown in Table 1 [4–6, 10–14, 19–24, 28], we summarize some reports on PDA in recent years briefly.

3 Nano-/microstructures of PDA

Owing to its robustness properties, PDA can be prepared as different nanostructures. To date, various types of PDA-derived nanocomposites have been reported. In this section, we mainly focus on the core@shell nanocomposites based on PDA surface modification.

3.1 Gold nanoparticles (AuNPs) and silver nanoparticles (AgNPs)

Gold (Au) and silver (Ag) NPs (AuNPs and AgNPs) exhibit strong antibacterial properties resulting from their extremely small size that allows them to efficiently penetrate bacterial cells in which they can cause serious adverse effects, predominantly via induction of oxidative stress, and thus are widely used for antibacterial purposes [36, 37]. They have attracted the attention of scientists due to their large surface area, favorable biocompatibility, surface modification versatility, and multivalent effects [38]. Additionally, AuNPs have other beneficial properties, such as non-toxicity, good biocompatibility, effective bactericidal activity, and high light stability [39], which have led to the development of AuNPs for biomedical applications. In addition, AuNPs are widely used in photothermal therapy applications due to their excellent localized surface plasmon resonance (LSPR) effect, which contributes to their unique optical properties. Samanta et al. [37] synthesized AuNP-decorated aragonite microdumbbells to enhance antibacterial activity. AgNPs have also been widely used in antibacterial products, which cause bacterial cell death through reaction with sulfur-containing proteins or sulfhydryl groups in the bacterial cell membranes. AgNPs have been widely used in the development of antimicrobial materials [40], due to their broad-spectrum antibacterial activity against Gram-positive and Gram-negative bacteria without causing antimicrobial resistance (Schemes 1 and 2).

Preserving the nanoparticles antibacterial properties when modifying AuNPs and AgNPs for antimicrobial applications is a challenge. PDA has received considerable research interest as a biomimetic polymer. PDA can be formed by self-polymerization in weak alkaline solutions at room temperature for the unique adhesion characteristics of

PDA [41]. The catechol group in PDA can reduce noble metal salts to metal NPs, which can then be immobilized on a scaffold to prevent their aggregation. PDA is quite hydrophilic due to its large number of catechol, quinine, and amine groups, which have made it increasingly popular as a universal surface modifier [41, 42]. The surface of PDA-modified membranes and the formed film show excellent antibacterial properties when they are fixed with AgNPs [42]. Moreover, since they are not sensitive to oxygen, AgNPs formed through the reduction of silver ions by catechol have a longer-lasting antimicrobial effect [43].

Zhang et al. [44] prepared excellent core-shell structure NPs (Au@PDA NPs) coated with PDA. Also, the nanofiber film was prepared by doping Au@PDA NPs into polylactic acid (PLA) for electrospinning and exhibited uniform size and good hydrophilicity. When the nanofiber membranes were soaked in a silver nitrate solution, the silver ion could be directly reduced to AgNPs in situ through the reduction potential of PDA. Owing to the unique adhesive properties of PDA, AgNPs can be effectively attached to the surface of the nanofiber membrane, thereby preventing their aggregation [43]. Furthermore, since the pores on the surface of the membrane are not blocked by the reductive AgNPs, the permeability of the membrane is not reduced and the hydrophilicity of the membrane is improved [41], thereby enhancing the bacteriostatic effect of the membrane. The procedure for preparing antimicrobial PLA-Au@PDA@Ag nanofibers is shown in Fig. 1. Briefly, the Au@PDA NPs were doped into PLA and stirred overnight, followed by electrospinning to obtain a smooth and uniform PLA-Au@PDA nanofiber. Then, the freshly prepared AgNO₃ solution was directly dropped onto the PLA-Au@PDA nanofibers where the silver ions were therefore reduced to AgNPs in situ through the reductive ability of the catechol group in the PDA.

The antibacterial activity of PLA-Au@PDA@Ag nanofibers against both *Escherichia coli* and *Staphylococcus aureus* was evaluated by determining the optical density absorbance of bacterial cell suspensions at 600 nm (OD_{600 nm}). *Escherichia coli* (*E. coli*) and *Staphylococcus aureus* (*S. aureus*) suspensions were treated with PLA-Au@PDA@Ag nanofibers, PLA, and PLA-Au@PDA membrane for 2, 4 and 6 h using PLA and PLA-Au@PDA membranes as the control groups. It was found that both PLA-Au@PDA and PLA-Au@PDA@Ag nanofibers have effective antibacterial activity against both *E. coli* and *S. aureus* cells. Moreover, compared with the PLA-Au@PDA nanofibers, the PLA-Au@PDA@Ag nanofibers showed significantly greater antibacterial activity through the in situ AgNPs on the surface of the PLA-Au@PDA@Ag nanofibers membrane [41]. Additionally, the bacterial reduction of PLA-Au@PDA and PLA-Au@PDA@Ag nanofibers also increased with the extension of time.

Table 1 Summary of polymerization, advantages, and applications of PDA

		Refs.
Polymerization	Under oxygen-containing conditions, dopamine monomers self-polymerize in an aqueous solution to form an oligomer, and high molecular weight PDA can be obtained through a cross-linking reaction	[10, 28]
Advantages	Simple preparation procedure Hydrophilicity Excellent biocompatibility Abundant active groups for easy functionalization Strong adhesion to both organic and inorganic surfaces Outstanding photothermal conversion effect	[4–6]
Applications	Construct of nano-/microcomposites Surface modification to obtain PDA-modified surfaces	[11–14] [19–24]

Collectively, PDA is a binder for various interfaces and effective anchoring groups, plays an important role in promoting the immobilization of AgNPs on PLA-Au@PDA nanofibers, and improves the hydrophilicity of PLA-Au@PDA@Ag nanofibers, which facilitates the release of Ag ions [43].

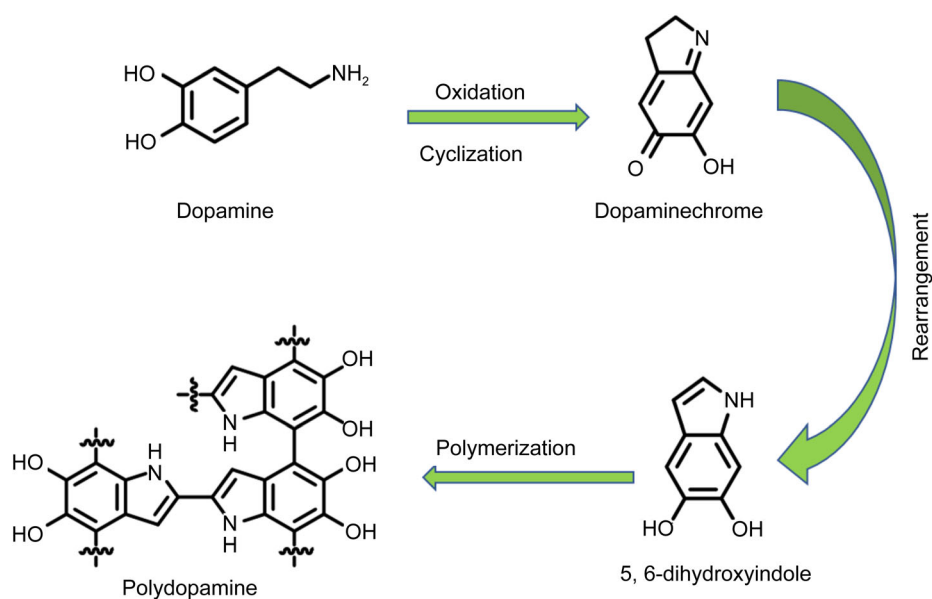
3.2 Fe₃O₄ nanoparticles

In recent years, nanostructured magnetic materials have been widely studied in the fields of nanotechnology research mainly due to their superparamagnetic property, which makes them to be easily collected and re-dispersed under an external magnetic field. Moreover, nanostructured magnetic materials have many other advantages, such as the nature of high magnetic saturation, good dispersibility, and easily modified surface. However, pure nanostructured magnetic materials easily agglomerate when directly exposed to biological systems. Many polymers have been synthesized and used to prevent the agglomeration and improve the biocompatibility by coating the polymers onto the magnetic nanoparticles, such as polyaniline [45], polypyrrole (PPy) [46], and PDA. DA can adhere to almost all material surfaces through oxidation and self-polymerization under alkaline conditions, which make it a multi-purpose intermediate layer to modify diverse substrates or nanostructures in order to endow or enhance certain specific functions [47]. In recent years, the development of PDA polymer decorated with magnetic NPs has rapidly advanced due to the higher degree of designability and flexibility in structures of PDA [11].

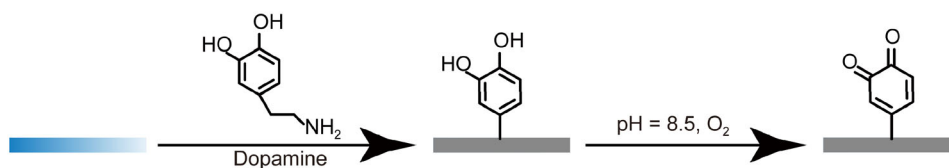
Besides, PDA has numerous functional groups, such as quinone, amine, and imine, which are beneficial for bonding metal ions or metal–ligand complexes, thus producing polymer–inorganic core/shell structures with adjustable functions [48]. Fe₃O₄ is one of the most frequently used metal oxides in PDA surface modification. As

a result of the intrinsic magnetism of Fe₃O₄, the PDA-modified Fe₃O₄ NPs can be easily collected and purified with an external magnetic field.

Yu et al. [2] grafted three-generation dendritic polyamidoamine G3 (PAMAM-G3) on the surface of Fe₃O₄@PDA to prepare multifunctional Fe₃O₄@PDA@PAMAM@NONOates nanocomposites. They modified PAMAM-G3 and N-diazeniumdiolates (NONOates) onto the Fe₃O₄@PDA core, which was used as a photoconversion agent to obtain the multifunctional Fe₃O₄@PDA@PAMAM@NONOates nanocomposites (Fig. 2a). Then, they studied the nitric oxide (NO) release behavior of the material under different laser irradiation conditions (Fig. 2c4), and the synergistic antibacterial activity of the photothermal and NO antibacterial against both Gram-negative *E. coli* and Gram-positive *S. aureus* (Fig. 2d). They first synthesized Fe₃O₄ clusters (Fig. 2b) by reducing FeCl₃·6H₂O in ethylene glycol in the presence of sodium acetate and sodium citrate using a one-pot hydrothermal reaction at 200 °C. Then, PDA was coated on the surface of the Fe₃O₄ clusters using a solution oxidation method. The obtained Fe₃O₄@PDA nanocomposites displayed a well-defined core–shell structure (Fig. 2b). They also investigated the photothermal effects of the Fe₃O₄ cluster, PDA NPs, Fe₃O₄@PDA, and Fe₃O₄@PDA@PAMAM-G3 in a phosphate-buffered saline (PBS) solution under irradiation with an 808-nm laser at a power of 0.5 W·cm⁻², using the PBS solution as a negative control. Noteworthy, since the PDA coating greatly enhances the photothermal effect of Fe₃O₄ clusters (Fig. 2c1), the temperature of Fe₃O₄@PDA was increased from 25 to 61.3 °C during 5-min irradiation. They also evaluated the synergistic antibacterial effect of the photothermal and NO effects against Gram-negative *E. coli* and Gram-positive *S. aureus* and found that the laser treatment greatly enhanced the antibacterial activity of Fe₃O₄@PDA@PAMAM-G3 through the photothermal effect of Fe₃O₄@PDA@PAMAM-G3,



Scheme 1 Oxidative polymerization of PDA. Reproduced with permission from Ref. [15]. Copyright 2015, Elsevier



Scheme 2 Modified surface with PDA

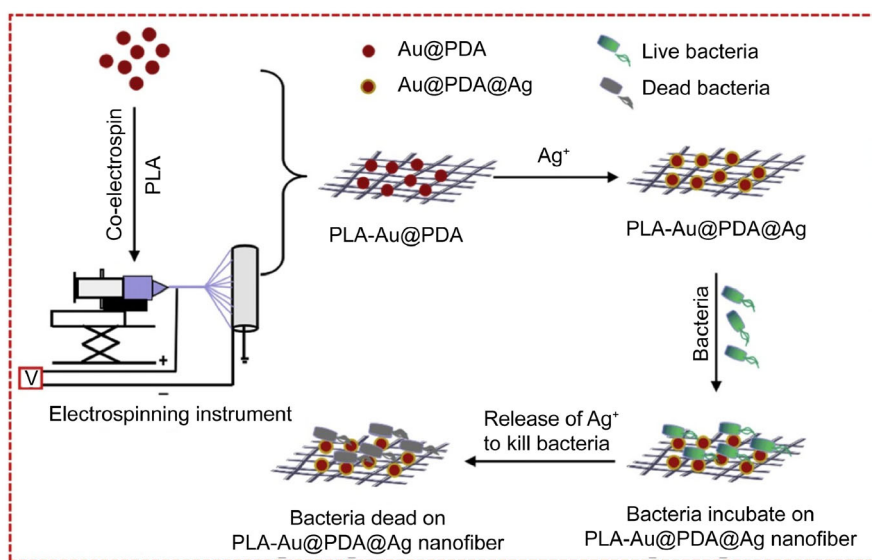


Fig. 1 Schematic diagram illustrating preparation of PLA-Au@PDA@Ag nanofibers and their antibacterial capacity. Reproduced with permission from Ref. [73]. Copyright 2019, Elsevier

which could rapidly increase the system temperature. The results in Fig. 2d show that for *S. aureus* bacteria, the viability was lower than 40% after laser irradiation.

3.3 SiO₂ nanoparticles

Silicon-based bioactive biomaterials, such as bioactive glass (BG, typical composition: SiO₂-CaO-P₂O₅), have

been extensively used for bone tissue repair due to their good biocompatibility, biodegradation, and tissue regeneration ability [49]. Monodispersed bioactive glass nanoparticles (BGNs) have been widely used for bioimaging, osteogenic differentiation of stem cells, drugs, and gene delivery for its enhanced biological performance [50]. Furthermore, nanoscale BG was found to be able to promote the healing of chronic wounds by enhancing angiogenesis [50]. Thus, various biodegradable nanocomposites based on BG NPs have been fabricated to meet the increased requirement of tissue repair and regeneration.

Inspired by mussels, PDA has been easily deposited on the surface of NPs, and the PDA functionalized NPs can be conjugated with other biopolymers through amidation or Schiff base reaction. As a result, we can prepare uniform multifunctional nanocomposites by PDA-based chemical modification [51].

Zhou et al. [52] developed a multifunctional bioactive nanocomposite hydrogel (FCB hydrogel, F: F127- ϵ -poly-L-lysine (FEPL); C: F127-Phe-CHO; B: BGN@PDA) through the click chemical cross-linking of FEPL, F127-Phe-CHO, and BGN@PDA. The hydrogel exhibited excellent self-healing and antibacterial properties against multidrug-resistant bacteria of skin tumor and wound healing. The synthesis process and application of the FCB hydrogel in tumor therapy and wound healing are shown in Fig. 3. In their strategy, BGN@PDA was designed to promote skin repair through the photothermal effect of PDA. Since the high antibacterial activity of EPL had already been reported, they used FEPL as a bactericide as well as to form a hydrogel network with F127-Phe-CHO and BGN@PDA through the Schiff base reaction [53]. The synthesis, physicochemical properties, and biomedical applications of the FCB hydrogel were subsequently investigated. As shown in Fig. 3a, the aldehyde group of F127-Phe-CHO and BGN@PDA was synthesized by F127-OTs, 4-hydroxybenzaldehyde, and self-polymerization of DA on the surface of BGN [54], respectively; the amino group of FEPL was synthesized by EPL. The FCB hydrogel was prepared through a Schiff base reaction between F127-Phe-CHO, BGN@PDA, and FEPL. Additionally, the in vivo antibacterial activity, NIR-induced photothermal tumor therapy, and wound healing property of the FCB hydrogel were also evaluated (Fig. 3a3).

The presence of BGN@PDA endowed the FCB hydrogel with an excellent photothermal performance; as a result, compared with the FCE hydrogel and H₂O, the temperature changes (ΔT) of the FCB hydrogel were increased by about 40 °C during 9 min under the same conditions (Fig. 3b1, b2). The results in Fig. 3b3–b5 demonstrate the excellent anticancer activity of the FCB hydrogel in vitro through the good photothermal therapeutic effect of FCB hydrogel due to the introduction of

BGN@PDA. Additionally, the excellent photothermal response of the FCB hydrogel was also beneficial to the antibacterial activity toward *E. coli*, *S. aureus*, and methicillin-resistant *S. aureus* (MRSA) in vitro and in vivo (Fig. 3c). The presence of BGNs in the FCB hydrogel enhanced the wound healing process by stimulating the formation of collagen and angiogenesis. In summary, the polypeptide-based nanocomposite hydrogel developed in this work could effectively promote skin repair and had excellent photothermal effect against bacterial infection and skin cancer. Additionally, the FCB hydrogel was demonstrated to be a promising candidate for anti-infection and wound healing.

3.4 ZnO nanoparticles

Although ZnO has good antibacterial activity, it is toxic to cell growth and tissue formation at large concentration, as high levels of Zn²⁺ induce reactive oxygen species (ROS), leading to oxidative stress and eventually cell death [55]. The proper amount of zinc, which can stimulate initial cell adhesion, spreading, proliferation, osteogenic differentiation, bone formation, and mineralization in vitro and in vivo, was needed on the biomaterial surface [56]. Therefore, it is critical to balance antibacterial activity and cytotoxicity by controlling the release of Zn²⁺ and generation of ROS by nanostructured ZnO. PDA has been widely used in the fabrication of multifunctional organic–inorganic materials for its excellent biocompatibility, biodegradation, and hydrophilicity [11, 13, 57]. In addition, PDA can scavenge ROS and is effective in promoting adhesion of many types of cells onto different substrates and can engage and activate integrin adhesion receptors on cells.

To balance the antibacterial activity and cytotoxicity ZnO nanorods (NRs), Li et al. [24] designed a hybrid of ZnO/PDA/RGDC NRs. The balancing mechanism of the bacteria–osteoblast race on ZnO/PDA/RGDC hybrid NR array-modified Ti in vivo is schematically illustrated in Fig. 4a. The ZnO NR arrays were modified by self-polymerization of DA and covalent immobilization of the RGDC peptide, as shown in Fig. 4b1, in which PDA was used to scavenge ROS generated by ZnO, as well as in combination with Zn²⁺ to reduce the concentration of released Zn²⁺ to improve the biocompatibility.

They prepared a uniform and narrow ZnO seed layer (ZnOs), with an average size of 20 nm prepared by atomic layer deposition (ALD) (Fig. 4b2). As revealed in Fig. 4b3, most of the ZnO NRs exhibit hexagonal rods with an average diameter of 100 nm (indicated by a red circle in the inset image in Fig. 4b3) growing along the near-perpendicular direction to the Ti substrate. The deposition of PDA covers the ZnO NRs, resulting in the disappearance of

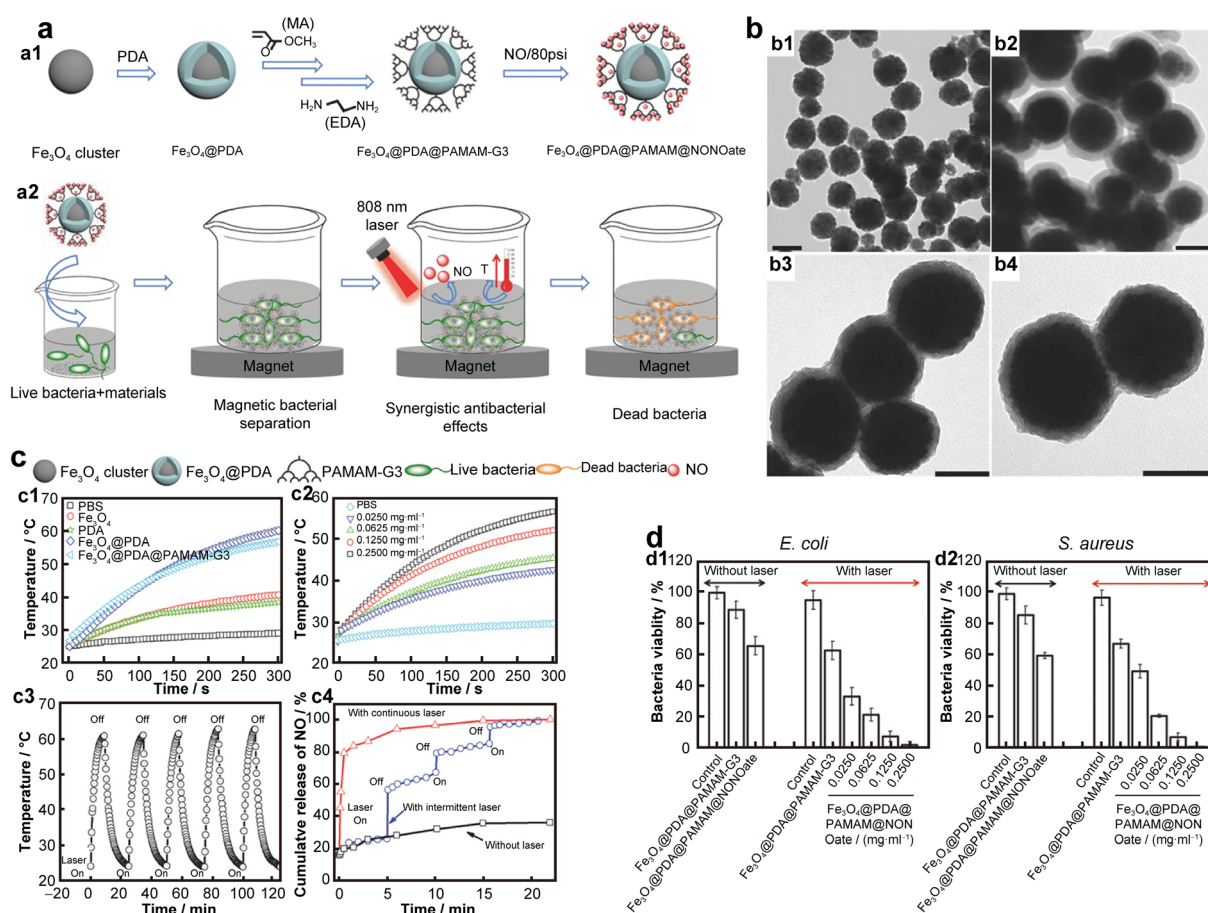


Fig. 2 **a1** Synthetic route of $\text{Fe}_3\text{O}_4@PDA@PAMAM@NONOate$; **a2** $\text{Fe}_3\text{O}_4@PDA@PAMAM@NONOate$ for magnetic separation, synergistic photothermal, and NO killing of bacteria; **b** transmission electron microscopy (TEM) image of **b1** Fe_3O_4 clusters, **b2** core-shell $\text{Fe}_3\text{O}_4@PDA$ nanocomposites, **b3** $\text{Fe}_3\text{O}_4@PDA@PAMAM-G3$, and **b4** $\text{Fe}_3\text{O}_4@PDA@PAMAM@NONOates$ (scale bars: 200 nm); **c1** photothermal effects of different nanomaterials under irradiation of 808-nm laser with a power density of $0.5 \text{ W}\cdot\text{cm}^{-2}$; **c2** concentration-dependent photothermal effect of $\text{Fe}_3\text{O}_4@PDA@PAMAM-G3$ under irradiation of 808-nm laser with a power density of $0.5 \text{ W}\cdot\text{cm}^{-2}$; **c3** photothermal stability evaluation of $\text{Fe}_3\text{O}_4@PDA@PAMAM-G3$ with five times laser switch-on and switch-off treatment; **c4** NO release profile of $\text{Fe}_3\text{O}_4@PDA@PAMAM@NONOate$ under different laser irradiation conditions; **d** bacterial viability of *E. coli* and *S. aureus* treated with $\text{Fe}_3\text{O}_4@PDA@PAMAM-G3$ and $\text{Fe}_3\text{O}_4@PDA@PAMAM@NONOate$ under different laser irradiation conditions. Reproduced with permission from Ref. [3]. Copyright 2018, Wiley Online Library

hexagonal NRs and a relatively rough surface morphology (Fig. 4b4). ZnO/PDA/RGDC NRs have an average length of $\sim 2 \mu\text{m}$ (Fig. 4b5) after covalent immobilization of the RGDC peptide (Fig. 4b6) whose distribution on the surface was confirmed by the distribution of sulfur in the elemental mapping image of Ti-ZnO/PDA/RGDC (Fig. 4b7).

The evaluation of the in vitro and in vivo antibacterial activity of the hybrid NR arrays against adherent *S. aureus* and *E. coli* by the live/dead (green/red) staining assay (Fig. 4c1) revealed the antibacterial activity of hybrid NR arrays. Compared to pure Ti, there are fewer red bacterial cells on the modified samples, indicating an antifouling and antibacterial activity of hybrid NRs against *S. aureus* and *E. coli*. As a supplement, the morphology of the adherent *S. aureus* and *E. coli* after incubation for 12 h on the modified

samples became more irregular or distorted compared with bacteria on Ti, as revealed by the field emission scanning electron microscopy (FESEM) images in Fig. 4c2. Moreover, the antibacterial activity of Ti-ZnO/PDA and Ti-ZnO/PDA/RGDC decreased slightly compared to that of the uncoated ZnO NRs, which is most likely due to that PDA can bind Zn^{2+} to reduce its toxicity.

They examined the cell morphology, cell adhesion, and cell spreading activity by staining F-actin fibers and nuclei with fluorescein isothiocyanate (FITC) and 4',6-diamidino-2-phenylindole (DAPI), respectively. As shown in Fig. 4d, after culturing for 1 day, compared with the poorly spread cells on Ti-ZnOs and Ti-ZnO, Ti-ZnO/PDA promoted cell extension and Ti-ZnO/PDA/RGDC showed improved cell spreading, growth. Additionally, filopodia and lamellipodia

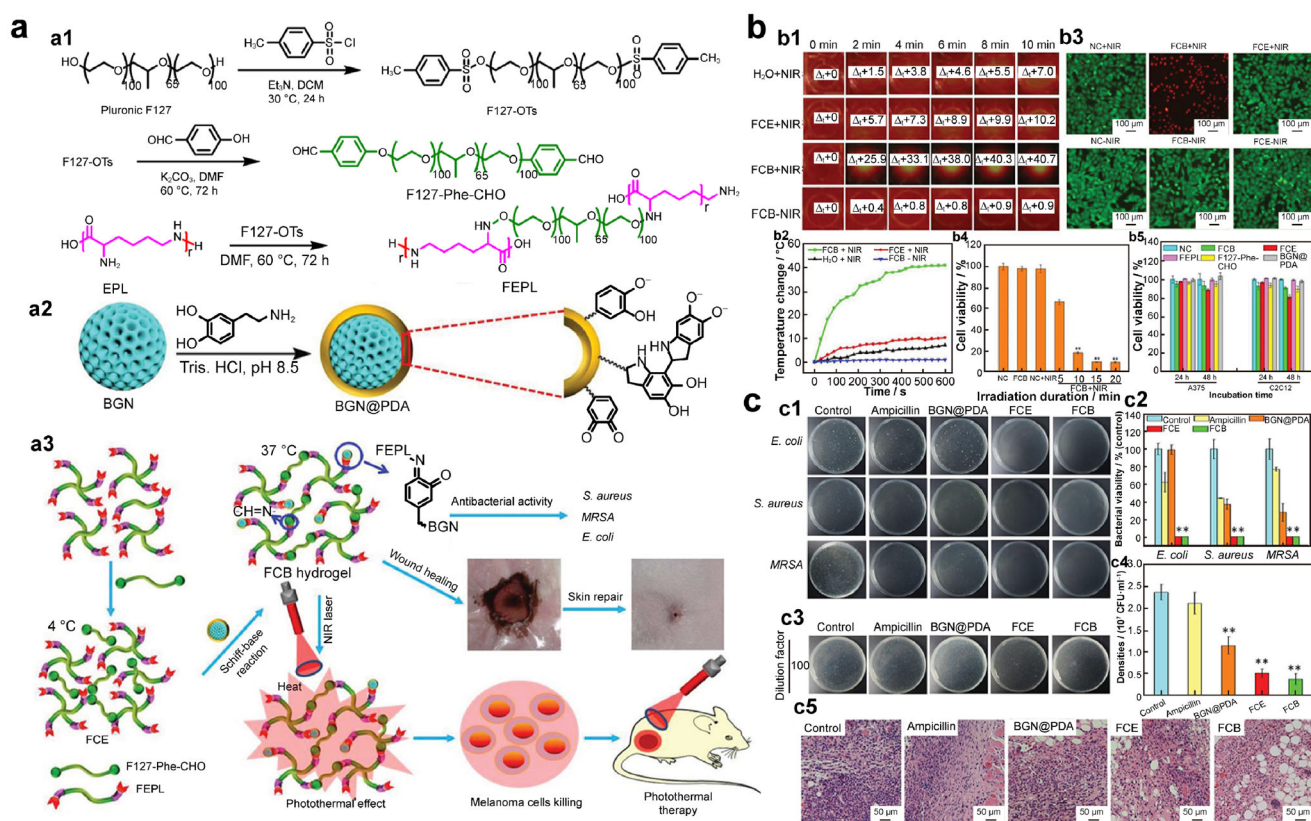


Fig. 3 a Scheme showing preparation and application of FCB hydrogel in tumor therapy and wound healing. Synthesis route of **a1** F127-OTs, FEPL and **a2** BGN@PDA, and **a3** schematic illustration for the formation of FCB hydrogel and bioapplication. **b** Photothermal performance and in vitro anticancer efficiency: **b1**, **b2** real-time infrared thermal images and photothermal heating curves of FCB hydrogel and controls with NIR irradiation (808 nm, $1.41 \text{ W}\cdot\text{cm}^{-2}$); **b3** in vitro anticancer efficiency of FCB hydrogel and controls with or without NIR treatment (808 nm, $1.41 \text{ W}\cdot\text{cm}^{-2}$, 10 min); **b4** FCB hydrogel under different irradiation durations (808 nm, $1.41 \text{ W}\cdot\text{cm}^{-2}$); **b5** cytotoxicity of FCB hydrogel and each composite in A375 and C2C12 cells. **c** Antibacterial activity in vitro and in vivo: **c1** pictures of colonies densities of *E. coli*, *S. aureus*, and MRSA treated with different samples; **c2** corresponding statistical data of colonies densities of *E. coli*, *S. aureus*, and MRSA treated with different samples; **c3** images of MRSA colonies growing on agar plates come from homogenized infected tissues after PBS buffer (control), ampicillin, BGN@PDA, and FCE and FCB treatments; **c4** quantitative bacterial colonies densities; **c5** optical images of H&E-stained tissue sections after treated with PBS buffer (control), ampicillin, BGN@PDA, FCE, and FCB, respectively. Reproduced with permission from Ref. [112]. Copyright 2019, Wiley Online Library.

can be observed in the cells on Ti-ZnO/PDA/RGDC, which indicates that Ti-ZnO/PDA/RGDC can promote bone cell adhesion and growth without apparent cytotoxicity.

Xiang et al. [58] developed an injectable hydrogel with dual-light irradiation with 808-nm NIR light (carbon quantum dots (CQDs) and PDA shown excellent photothermal performance with 808-nm NIR light) and 660-nm red light (CQD-decorated ZnO (C/ZnO)-generated ROS with 660-nm red light). As shown in Fig. 5a, the hydrogel, named DFT-hydrogel, was formed by the combination of Zn^{2+} with folic acid (FA) and PDA. The DFT-C/ZnO-hydrogel has a strong photothermal effect and good photostability (Fig. 5b). Figure 5c reveals that DFT-C/ZnO-hydrogel possesses highly efficient antibacterial ability, due to the outstanding photodynamic and

photothermal properties under 660- and 808-nm dual-light irradiation for the existence of PDA and CQDs.

Biomaterials with proper zinc can stimulate initial cell adhesion, spreading, proliferation, osteogenic differentiation, bone formation, and mineralization in vitro and in vivo. Although it has been reported that nanostructured ZnO has good antibacterial activity, there is obvious cytotoxicity when a large concentration of Zn^{2+} produces adverse effects on cell growth and tissue. It is a wise choice to chelate Zn^{2+} with PDA to form metal-ligand coordination to control the release of Zn^{2+} and enhance the biocompatibility.

As mentioned above, PDA has attracted heightened research interest in various antibacterial nano-/micromaterials because of its excellent performance. For example,

PDA endows nanoparticles with photothermal effect and prevents the aggregation of nanoparticles to keep original properties. More than anything, the addition of PDA will not increase biotoxicity of the composite. Therefore, PDA provides a novel approach for the construct of nanocomposites. The effects of PDA in antibacterial nano/microstructures are summed up in Table 2 [2, 24, 41, 43–45, 50, 51, 57].

4 Surface modification of PDA

Implant infections and failure of medical devices due to bacterial adhesion and growth on their surfaces pose serious public health threats. Therefore, it is of significant importance to develop antibacterial surfaces that can prevent bacterial attachment and biofilm formation, particularly for biomedical applications. As a result, PDA has increasingly attracted considerable attention due to its ability to adhere to various surfaces.

4.1 Stainless steel (SS)

The most common material in orthodontic appliances is stainless steel (SS), whose surface modification against bacterial colonization is mainly achieved through passive resistance and active attack. Passive resistance approaches include the use of hydrophilic surface against bacterial colonization by inhibiting bacterial adhesion [59], while active attack approaches mainly refer to the use of bactericides aimed at killing bacteria. Currently, PDA-coated materials are widely prepared by grafting various molecules and polymers on them to obtain materials with stable and durable surface modification for use in diverse applications [3].

Lee et al. [60] used PDA as the adhesion layer to promote the adhesion of the polymer poly(3,4-ethylenedioxythiophene) (PEDOT) onto the SS surface. As shown in Fig. 6a, a zwitterionic poly(EDOT-phosphorylcholine) (PC) coating with AgNPs was developed to achieve both antifouling and antibacterial effects, in which AgNPs were

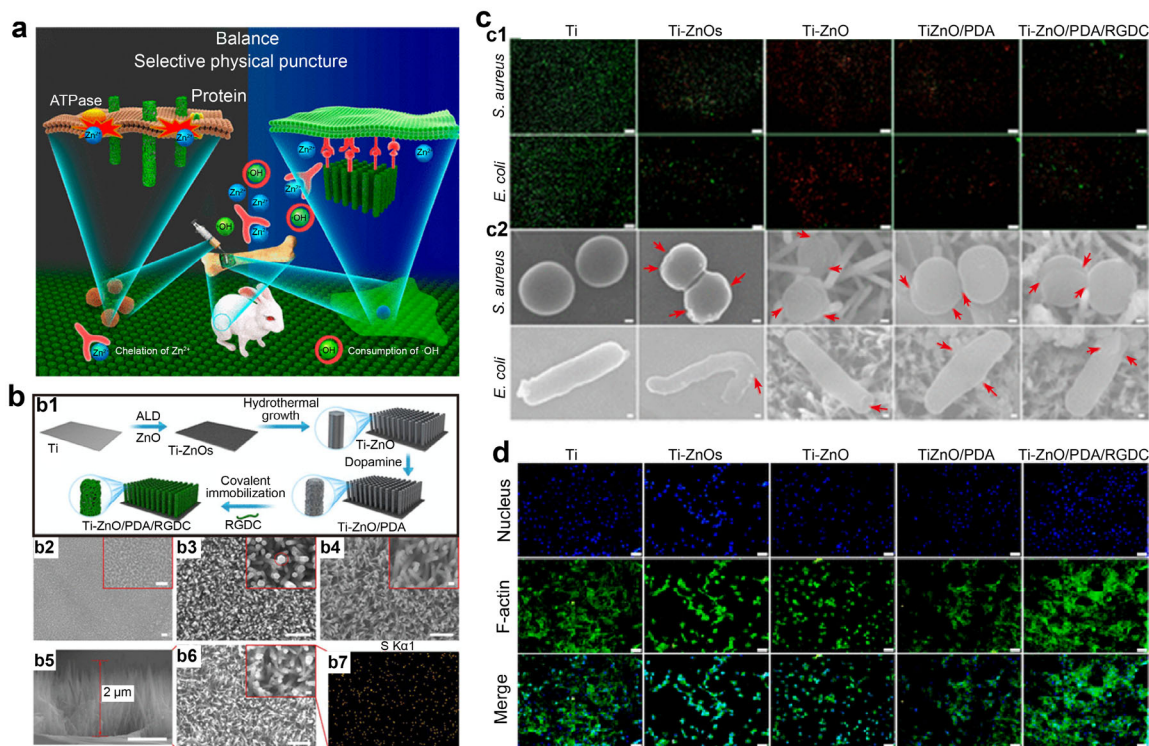


Fig. 4 a Schematic illustration of balancing bacteria–osteoblast competition on titanium modified with ZnO/PDA/RGDC hybrid NR arrays in vivo. **b1** Schematic illustration of fabrication process of the hybrid ZnO/PDA/RGDC NR arrays on Ti; field emission scanning electron microscope (FESEM) images of **b2** Ti-ZnOs, **b3** Ti-ZnO, **b4** Ti-ZnO/PDA, and **b6** Ti-ZnO/PDA/RGDC; **b5** cross-sectional image; **b7** elemental mapping of Ti-ZnO/PDA/RGDC (scale bar: 100 nm; inset scale bar: 1 μ m). **c1** Fluorescent images of stained bacteria after treatment on various surfaces for *S. aureus* and *E. coli* (scale bars: 50 μ m); **c2** FESEM morphology of *S. aureus* and *E. coli* seeded on various surfaces (scale bars: 100 nm); **d** fluorescent images of MC3T3-E1 cells cultured on different samples for 24 h with F-actin stained with fluorescein isothiocyanate (FITC, green) and nuclei stained with 4',6-diamidino-2-phenylindole (DAPI, blue) (scale bars: 50 μ m). Reproduced with permission from Ref. [29]. Copyright 2017, American Chemical Society

reduced from Ag^+ by PEDOT [61]. They chose PDA as the first layer due to its strong adhesion capability on the metal substrate, followed by poly(EDOT-OH) to assist the adhesion and grafting of the poly(EDOT-PC) layer.

To evaluate the antifouling and antibacterial activity of the modified SS surface, the bacteria washed from the surface were cultured on tryptic soy agar (TSA) plates and the surfaces were stained using the LIVE/DEAD BacLight Bacterial Viability Kit (Thermo Fisher Scientific Inc., Waltham, MA, USA) to observe the bacterium by confocal laser scanning microscopy (CLSM). Compared with the other five groups, a significantly larger amount of *E. coli* were washed off the SS-DO-OH-PC plate, indicating that the pathogens were easily washed off from the SS-DO-OH-PC as a result of the antifouling activity of poly(EDOT-PC) (Fig. 6b). Meanwhile, both SS-DO-OH-Ag and SS-DO-OH-PC-Ag were effective against *E. coli* after incubation for 3 h, due to the antibacterial activity of Ag^+ and AgNPs (Fig. 6c). The CLSM images revealed similar results (Fig. 6d, e). This study demonstrated the feasibility of a method developed to form a durable antifouling and antibacterial nanocomposite coating for SS in orthodontic appliances through the layer-by-layer deposition of PDA, poly(EDOT-OH), poly(EDOT-PC), and AgNPs.

Zhang et al. [62] coated PDA on the SS substrate to improve the adhesion, hydrophilicity, and reactivity of the substrate, followed by the co-deposited of TiO_2 -PTFE onto the PDA sublayer (Fig. 6f). Figure 6g, h indicates that the TiO_2 -PTFE-1-coated surface exhibited the lowest bacterial adherence compared with the uncoated 316L SS surface. As a result, the combination of sol-gel coating technique

and PDA surface functionalization can improve the antibacterial and anti-adhesion properties of 316L SS.

SS implants have been designed to provide internal support to biological tissues and used extensively in dental, endovascular, and orthopedic surgery. However, the problem of bacterial attachment and long-term presence of metal devices in the body is associated with an increased risk of corrosion and contamination, leading to an increase in inflammatory responses. Introducing antibacterial agents using PDA on the surfaces of SS implants is simple and effective in fighting bacterial infections.

4.2 Titanium implants

Currently, implantable medical devices have been frequently used in the treatment of bone and periodontal diseases [63]. Titanium implants, due to their benefits, including corrosion resistance, mechanical strength, and excellent biocompatibility, account for a large portion of the market of orthopedic and dentistry implant prostheses. Unfortunately, patients are increasingly threatened by implant-associated infection. For instance, after implanted and exposed to body fluids, titanium materials tend to absorb proteins and lead to undesirable infection [64]. Even worse, fouling on the surface of implants may cause the formation of biofilms, which mainly contribute to the failure of antibiotics [65]. Consequently, it is of urgent necessity to decrease bacterial fouling and prevent biofilm formation [66].

As mentioned above, titanium implants need to be endowed with antibacterial and antifouling properties. It is

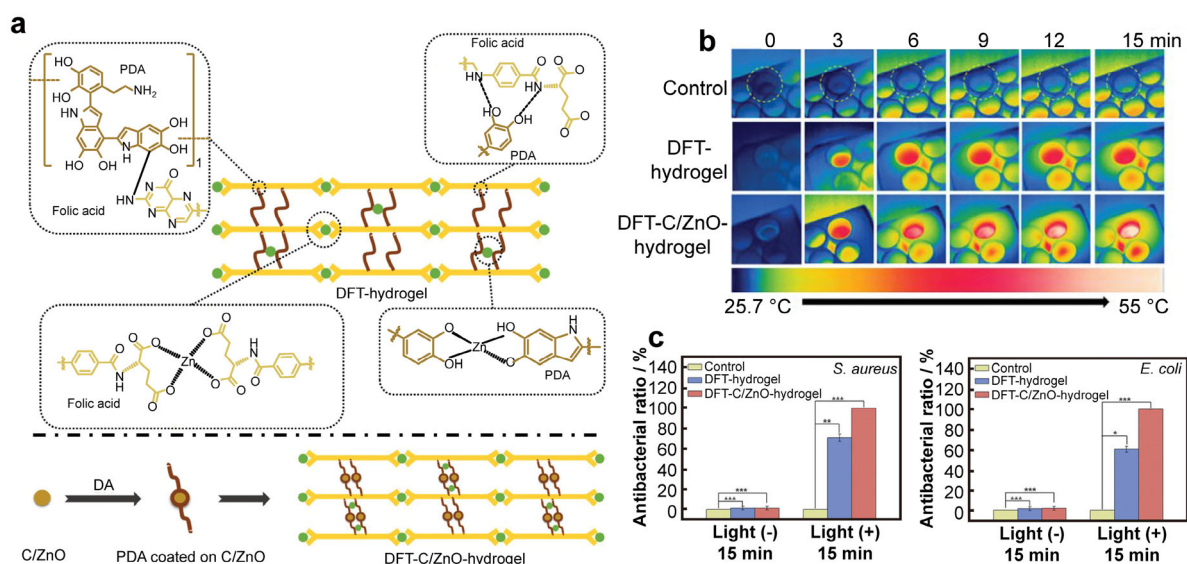


Fig. 5 a Schematic illustration of molecular structure of the hydrogels; b real-time infrared thermal images of different hydrogels under 660- and 808-nm mixed light irradiation; c antibacterial ratio of different hydrogels against *S. aureus* and *E. coli*. Reproduced with permission from Ref. [139]. Copyright 2019, Wiley Online Library

Table 2 Effects of PDA in antibacterial nano-/micromaterials

Kinds of nano-/micromaterials	Effects of PDA	Refs.
AuNPs/AgNPs	Inducing chemical reduction of silver and gold ions Improving hydrophilicity of nanomaterial Preventing aggregation and suppressing leaching out of nanoparticles to maintain antibacterial ability	[41, 43]
Fe ₃ O ₄	Endowing nanoparticles with photothermal antibacterial effect Preventing agglomeration when directly exposed to biological systems and improving the biocompatibility Serving as a versatile platform for Fe ₃ O ₄ to deposit on surfaces by in situ nucleation	[2, 44, 45]
SiO ₂	Increasing toughness to use for requirement of tissue repair Offering photothermal antibacterial effect	[50, 51]
ZnO	Controlling release of Zn ²⁺ via chelation between PDA and Zn ²⁺ , further enhancing biocompatibility Reducing amount of ROS produced by ZnO through radical scavenging of PDA Chelating Zn ²⁺ to form metal–ligand coordination and prepare hydrogels to increase retention on wounds	[24, 57]

well known that the traditional antibiotic gentamicin is indeed effective in fighting against both *E. coli* and *S. aureus*, and polyethylene glycol (PEG) is often used for antifouling [65, 67]. Accordingly, Zeng et al. [67] designed and synthesized several branched polymeric agents, individually designated as EPEG, GPEG, and GEG (Fig. 7a), using a one-pot ring-opening reaction of gentamicin with PEG species in order to simultaneously prevent bacteria growth and fouling. They obtained GEG from gentamicin with amino groups and the ethylene glycol diglycidyl ether (EGDE) with the di-epoxide groups and acquired GPEG from gentamicin and another di-epoxide compound, namely polyethylene glycol diglycidyl ether (PEGDGE). For comparison purpose, EPEG was reacted from ethylenediamine and PEGDGE, which rendered only antifouling effect. Then, the polymers were coated on titanium disks pretreated with PDA.

CLSM and scanning electron microscope (SEM) images showed the antibacterial and antifouling activity of the polymer coatings on the surface of titanium disks (Fig. 7b). Specifically, in the control groups, when *S. aureus* and *E. coli* were incubated with Ti disks or Ti-EPEG, only the green fluorescence staining can be observed, which demonstrates that Ti disks alone are totally incapable of killing bacteria and the gentamicin provides the antibacterial activity. In contrast, nearly all the bacteria stained red, indicating that Ti-GEG and Ti-GPEG have excellent antibacterial activity. As the live/dead fluorescence staining images, the SEM images provided the same evidence. Regular morphology and smooth surface are visible in the groups of Ti disks and Ti-EPEG, but the antibacterial effect of Ti-GEG and Ti-GPEG made the membrane collapse and

the shape change in the images of both *S. aureus* and *E. coli*. Moreover, there are fewer bacteria on the surface of Ti disks containing PEG (Ti-EPEG, Ti-GEG, and Ti-GPEG). These experimental results compellingly confirmed the antifouling activity of the synthesized materials. To sum up, new capabilities against not only bacterial but also fouling can be endowed on Ti disks by decorating functional polymers.

Lee et al. [68] succeeded to connect antibiotics with Ti surfaces. Based on the carboxyl groups on antibiotics, PDA existing on the surfaces of Ti tends to offer abundant amino groups to graft antibiotics. For instance, as shown in Fig. 8a, at room temperature, ceftazidime (CFT) was fixed on Ti substrates coated by PDA/polyethyleneimine (PEI) using chemical reaction. While at 37 °C, because of the hydrolyzation of the amido bonds, CFT could be released quickly under acidic condition to realize antibacterial effect against both Gram-positive and Gram-negative bacteria. After exposure to bacterial suspension for 24 h, the antibacterial activities of Ti, Ti-DP, and Ti-DPC were evaluated by SEM photographs and disk assay. In Fig. 8b, remarkable inhibiting effect can be observed. This was mainly attributed to adhesive resistant coating added to the surfaces, such as PDA and cationic polymer PEI. They are able to hinder the bacterial colonization and restrain the formation of biofilm. Owing to the positive charge on PEI, Ti modified by PEI exhibited slight inhibition, while the effect of Ti-DPC was the most obvious against whether *Pseudomonas aeruginosa* (*P. aeruginosa*) or *S. aureus*. In Fig. 8c, d, compared to the control groups, two kinds of microorganism were apparently eliminated under the effect of modified Ti surfaces after 12 h. And the difference

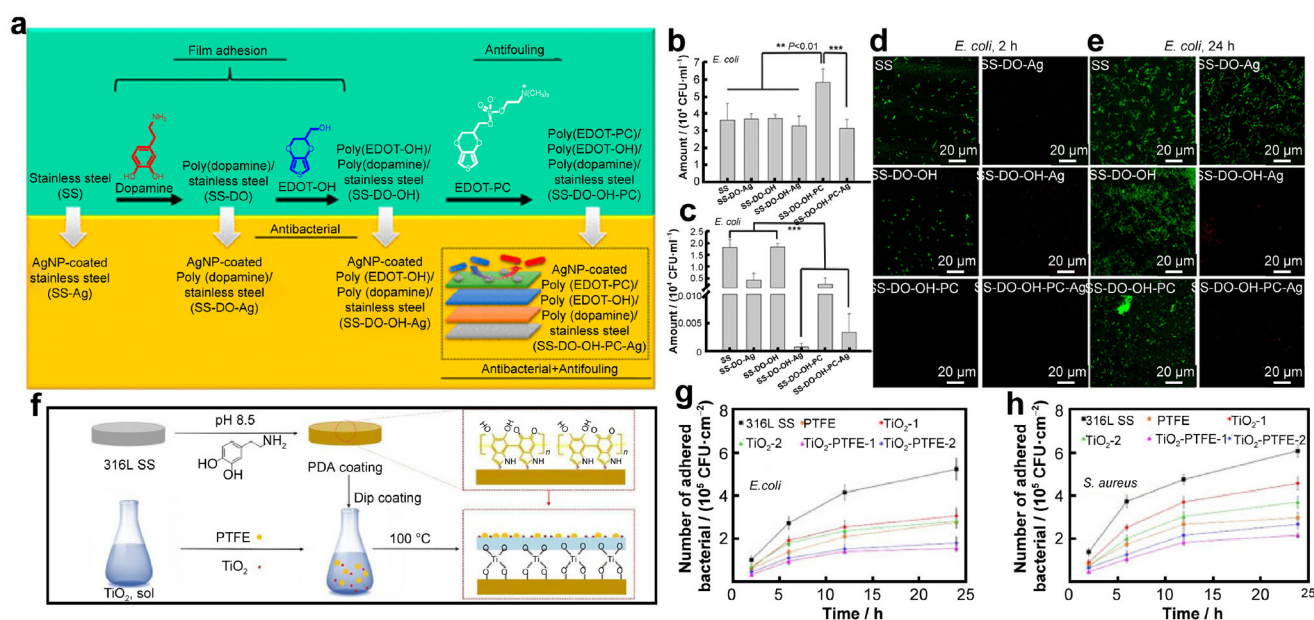


Fig. 6 a Design of antibacterial and antifouling SS: deposition of polydopamine and poly(EDOT-OH) for adhesion enhancement, deposition of zwitterionic poly(EDOT-PC) for antifouling of surface, and deposition of silver nanoparticles (AgNPs) for antibacterial coating; **b** amounts of *E. coli* (in colony-forming unit, CFU·ml⁻¹) obtained after washing with PBS and culturing on TSA; **c** amounts of *E. coli* (in CFU·ml⁻¹) in culture medium after incubation for 3 h; **d** CLSM images after 2-h *E. coli* adhesion, where prominent green fluorescence was found in SS and SS-DO-OH groups; **e** CLSM images after 24-h *E. coli* adhesion, where only SS-DO-OH-Ag and SS-DO-OH-PC-Ag groups exhibited scarce green fluorescence. Reproduced with permission from Ref. [142]. Copyright 2019, American Chemical Society. **f** Coating process of the TiO₂-PTFE on PDA-modified 316L SS; adhesion of **g** *E. coli* and **h** *S. aureus* to different samples at different time. Reproduced with permission from Ref. [144]. Copyright 2019, Elsevier

became more evident after 24 h. These data indicated that CFT was well grafted on Ti hybrids and effectively prohibited bacterial colony growth.

Ti implants, as a kind of the most common instruments, play an irreplaceable role in modern medical treatment. However, more and more concerns have been shown to the discussion of the contamination of Ti implants. Researches on how to realize antibacterial and antifouling effects and maintain intrinsic properties really make sense.

4.3 Biomedical catheters

Catheter-related infections (CRIs) are a kind of nosocomial infections that cannot be neglected due to their high mortality. Patients develop CRIs possibly through the introduction of pathogens in the urinary tract, blood, and lung tissue. In the clinical treatment, CRIs occur frequently, which is attributed to the increasingly extensive use of biomedical catheters (BCs). BCs are irreplaceable in many medical applications, such as fluid discharging, blood indwelling, and mechanical ventilation. Connecting the body with an external complex environment, BCs are prone to be contaminated by pathogenic microorganisms and even biofilms [69, 70], which undoubtedly impedes the utilization of BCs and poses a serious threat to the patient's health.

In this exciting research field, Yu et al. [71] developed a facile and effective strategy for antibacterial and antifouling coating. Sulfamethoxazole (SMZ) and trimethoprim (TMP) are two commercial antibiotics, showing powerful antibacterial effect against both Gram-positive and Gram-negative bacteria. However, their tendency to spontaneously form large particles in aqueous solution limits the application of SMZ and TMP. Inspired by microcrystalline drugs, as previously reported [72], these authors transformed SMZ and TMP into crystalline powder in order to increase their absorption rates. After depositing SMZ and TMP on the surface of BCs in a form of microcrystal, the antifouling agent PEG was then added into the system via Schiff base reaction with PDA, and this created a hydrophilic environment that is unfavorable for the adhesion of microorganisms (Fig. 9a) [1, 73]. This preparation method is simple and efficient, and in this way, the coating on BCs simultaneously integrated bactericidal activity with antifouling property. Surprisingly, the combined use of SMZ and TMP may be expected to decrease bacterial drug resistance.

SEM and dynamic light scattering (DLS) data revealed the necessity of preparing microcrystalline SMZ and TMP. As shown in Fig. 9b1, large blocks can be clearly seen. In comparison, processed SMZ and TMP particles are not merely smaller than the original ones but also have more

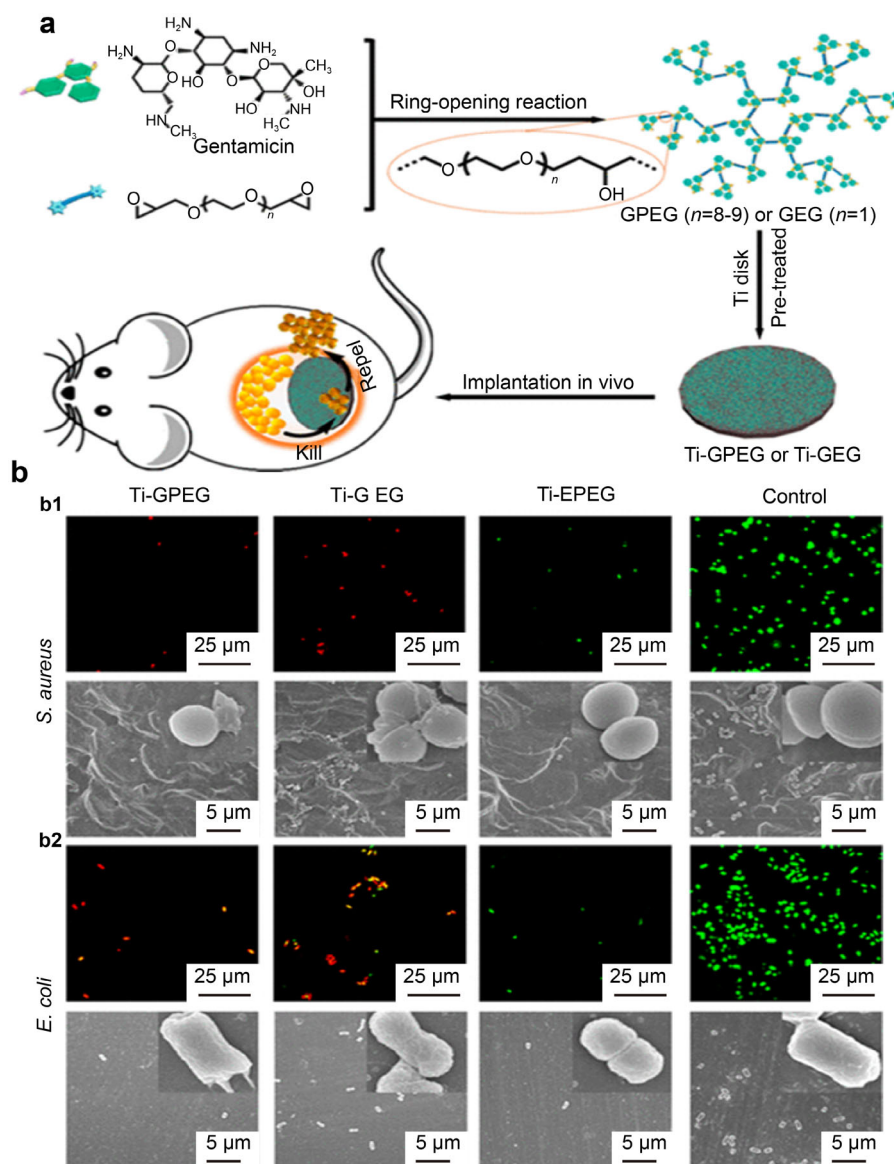


Fig. 7 **a** Schematic illustration of synthetic route of antibacterial and antifouling polymeric agents and their application for surface functionalization of medical implants; **b** CLSM and SEM images of *S. aureus* **b1** and *E. coli* **b2** on modified Ti disks. Reproduced with permission from Ref. [155]. Copyright 2018, American Chemical Society

regular shapes (Fig. 9b2). The ratio of microcrystalline SMZ and TMP is set at 5:1, which is the optimum ratio in clinical application. Inhibition efficiencies against two kinds of pathogens, namely *S. aureus* and *E. coli*, are shown in Fig. 9b3. The minimum inhibitory concentration (MIC) value of either the microcrystalline drug or the pristine drug is 512 and 4096 $\text{ng}\cdot\text{ml}^{-1}$, respectively, against *S. aureus* and *E. coli*, demonstrating that the microcrystallization has negligible effect on the antibacterial effect. Similarly, the results of the live/dead fluorescence staining assay also indicate the antibacterial activity of drugs by the higher number of red fluorescence-stained cells (representing the dead bacterial cells) than the

control group (Fig. 9c). Regarding the other aspect, we noticed that there was no clear distinction in the number of bacteria on the surfaces of BC drugs and pristine BC, while fewer fluorescence bacterial cells on the BC-PEG drugs surface confirm the effectiveness of PEG. In a word, the obtained system that connects BCs with PEG drugs by PDA has excellent antibacterial and antifouling properties.

4.4 Fabric

With the progress of modern medicine, traditional pure cotton products have been substituted by medical

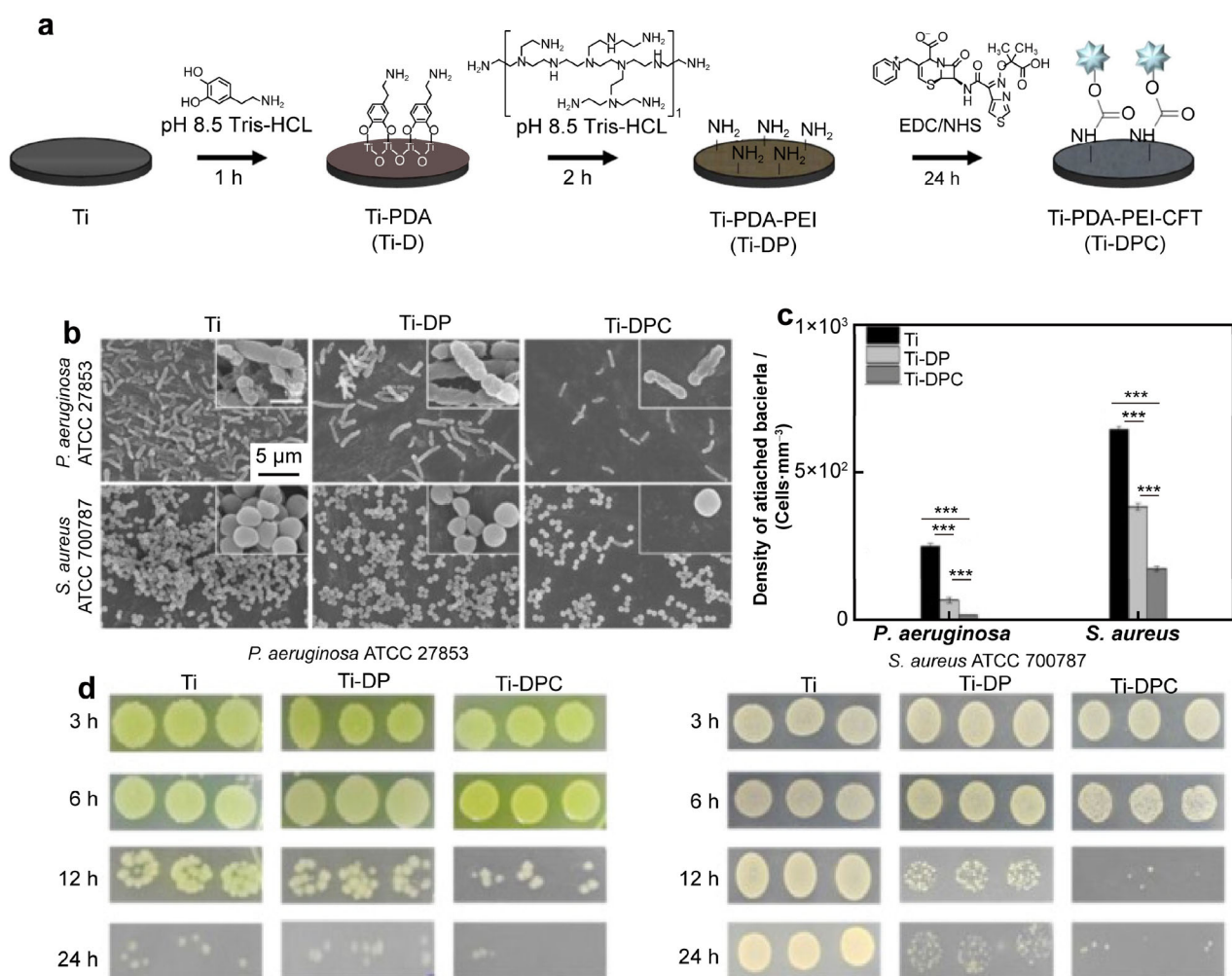


Fig. 8 **a** Schematic illustration of modification of titanium surface; **b** SEM images of two kinds of bacterial binding on specimens; **c** antibacterial activities by disk assay of Ti, Ti-DP, and Ti-DPC after 24 h; **d** photographs of viable bacteria after incubation for different times. Reproduced with permission from Ref. [156]. Copyright 2019, Elsevier

nonwoven fabrics due to their advantages, including short production process, sterilization convenience, outstanding application versatility, and easy to combine with other materials [74]. Although the nonwoven fabrics are sterilized before use, there is still a risk of serious infection due to their direct exposure to wounds. Photodynamic therapy (PDT) is an emerging treatment modality, where a photosensitizer and oxygen generate one or several kinds of ROS under irradiation. Compared to traumatogenic therapy, PDT causes minimal traumas, or even noninvasive, which makes it receive much attention and be applied in clinical practice. On the basis of the above findings, a coating sensitizer on medical nonwoven fabrics offers a novel strategy to prevent and treat microbial infections.

Zhu et al. [75] combined the commercial sensitizer eosin Y (EY) with quaternary ammonium (QA) to prepare several innovative cationic polymers (EY-QEGED-R,

R = $-C_6H_{13}$ or $-CH_3$) based on the ring-opening reaction (Fig. 10a). Then, these compounds were coated on nonwoven fabrics with the aid of PDA to obtain multifunctional systems that achieve synergetic antibacterial and antifouling effects under light irradiation. As shown in Fig. 10b, both Gram-negative (*E. coli*) and Gram-positive (*S. aureus*) bacteria can be distinctly destroyed according to the red fluorescence. The fact that the EY-EGED group under irradiation shows some dead bacteria confirms the powerful antibacterial property of PDT, while the EY-QEGED- CH_3 and the EY-QEGED- C_6H_{13} groups without light irradiation represent the bactericidal activity of QA. Unsurprisingly, the combined application of PDT and QA would generate more satisfactory antibacterial data. Similarly, SEM images revealed the bacterial morphological difference between the variously treated groups. It is surprising though that the nonwoven fabrics coated with PDA

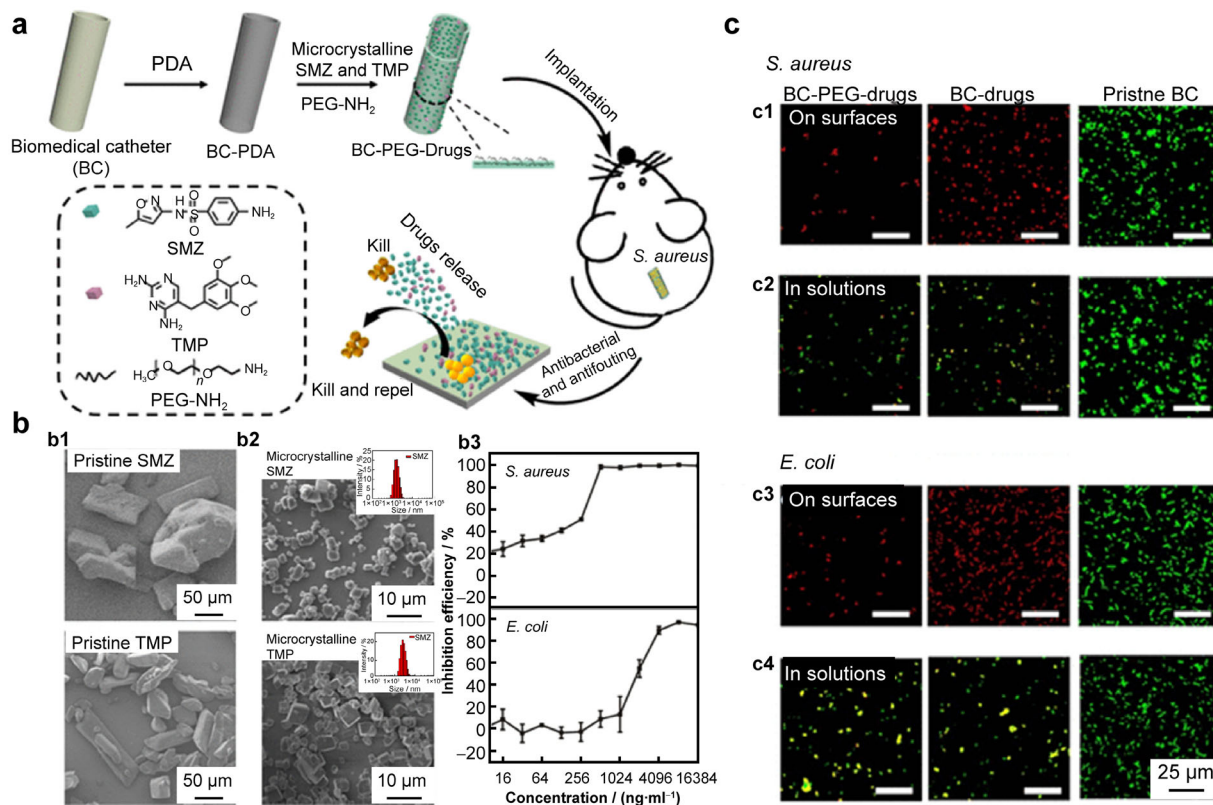


Fig. 9 a Schematic illustration of modification route of biomedical catheters and resultant antibacterial characteristics; **b1** SEM images of pristine SMZ and pristine TMP in water; **b2** SEM images and size distributions of microcrystalline SMZ and microcrystalline TMP; **b3** inhibition efficiencies of antibacterial microcrystalline SMZ-TMP against *S. aureus* and *E. coli*, respectively; antibacterial activities of **c1** *S. aureus* and **c2** *E. coli* after 8-h incubation; fluorescence images of live/dead fluorescence staining assay for bacteria cells **c1**, **c2** on surface and **c3**, **c4** in solution (scale bars: 25 μm). Reproduced with permission from Ref. [160]. Copyright 2019, American Chemical Society

alone retained more bacteria than the ones coated with polymers, confirming that the EY-based polymers are stain resistant to a certain extent.

Inspired by the promising antibacterial results of the polymer coatings, the authors then developed and used an experimental model of infected wounds on the dorsal side skin to determine the availability of materials in vivo (Fig. 10c). After treatment with *S. aureus*, some wounds were covered with modified nonwoven fabrics. Compared with the treatment groups, the infection group without any other operation showed larger wound area and more bacterial colonies after 14 days. Therefore, this rational design of wound dressing provides an effective method to inhibit infection and accelerate healing.

5 Summary and outlook

PDA can be easily produced by the self-polymerization of DA. Its size, shape, and morphology can be readily adjusted by controlling the reaction conditions. PDA-based materials have interesting properties, including good metal

coordination capacity, excellent biocompatibility and biodegradability, strong quenching effect, and outstanding photothermal conversion ability. The understanding of these interesting properties has been used to design more coating strategies and led to various applications of PDA in nanomedicine, including antibacterial treatment. Although in the past few years, an impressive amount of studies have accumulated on this topic, transferring the applications of PDA from the research laboratory into real-world applications seems somewhat unrealistic at this moment, due to the existence of some major issues that should be primarily addressed. Moreover, establishing how to precisely control the PDA deposition on the substrates will have a profound effect on the construction of functional materials with optimal properties. Additionally, some crucial issues, such as long-term stability and toxicity during the retention of PDA in the organism, should be taken into account when dealing with its applications in biology, biotechnology, and medicine. Especially in biomedicine-related fields, biomedical applications of PDA require a detailed understanding of its interactions with biological system.

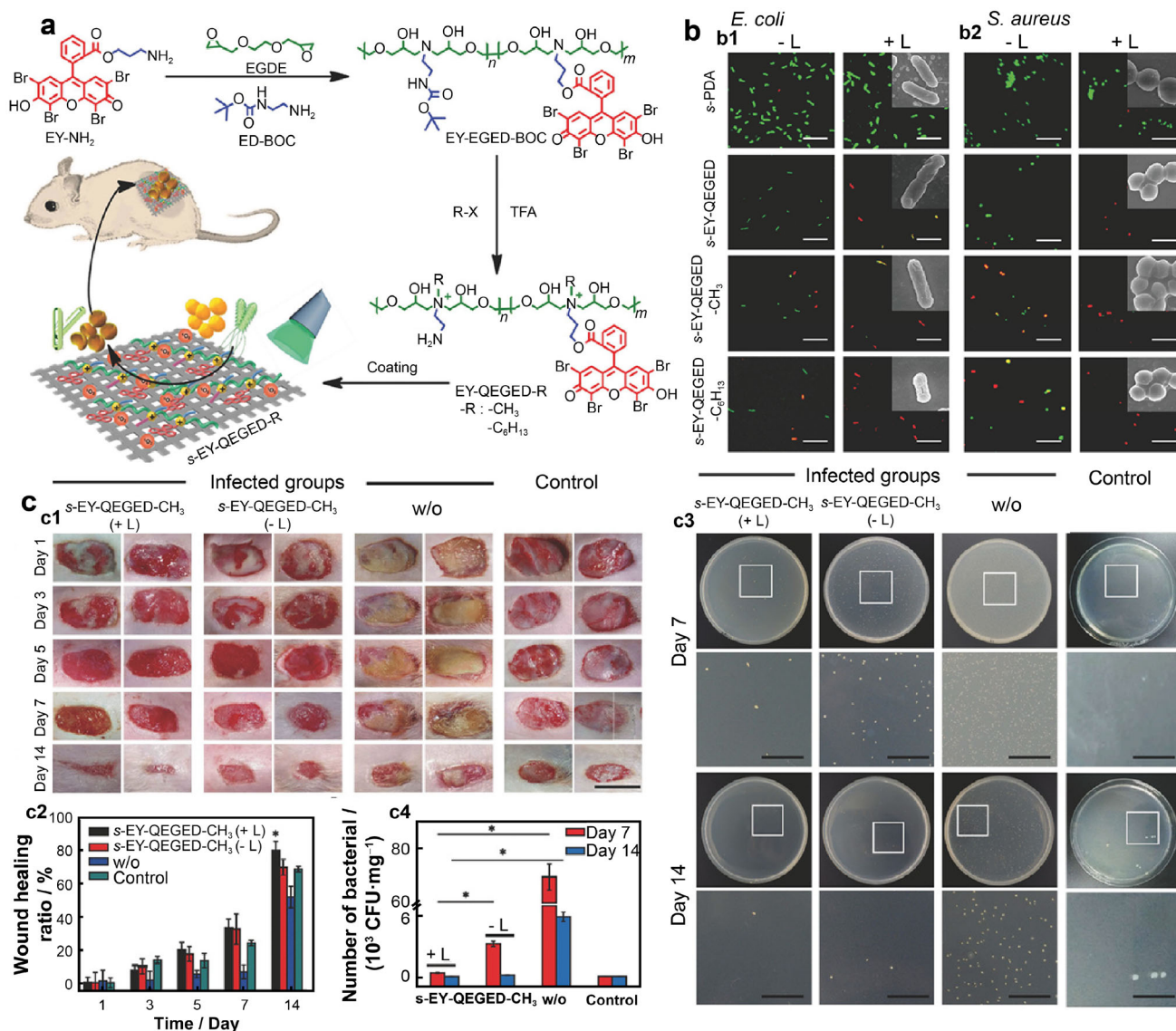


Fig. 10 **a** Schematic illustration of synthetic route of polycationic antibacterial agents with multiple functional components and a “proof-of-concept” application as wound dressing material; **b** antibacterial activities against **b1** *E. coli* and **b2** *S. aureus* on pristine s-PDA and polymer-coated surfaces using live/dead bacterial viability assay, where insets of two columns with light shining show SEM images of *E. coli* and *S. aureus* on each modified surface (scale bars: 5 μm); **c1** photomicroscopic images and **c2** ratio of wound healing of rat model for 1–14 days; **c3** photomicroscopic images and **c4** bacteria number of bacterial colony-forming units obtained from different tissues of rats treated under various conditions (scale bars: 1 cm). Reproduced with permission from Ref. [168]. Copyright 2018, Wiley Online Library

In conclusion, the research of PDA has a very bright future in antibacterial applications due to its ease of use combined with fascinating properties. Once the aforementioned issues can be successfully addressed in the near future, we believe that PDA will provide scientists new tools to overcome long-standing practical scientific challenges.

Acknowledgements This study was financially supported by the National Natural Science Foundation of China (Nos. 21875014 and 52073013).

Declarations

Conflict of interests The authors declare that they have no conflict of interest.

References

- [1] Brown ED, Wright GD. Antibacterial drug discovery in the resistance era. *Nature*. 2016;529(7586):336.
- [2] Yu SM, Li GW, Liu R, Ma D, Xue W. Dendritic Fe₃O₄@poly(dopamine)@PAMAM nanocomposite as



- controllable no-releasing material: a synergistic photothermal and no antibacterial study. *Adv Funct Mater.* 2018;28(20):1707440.
- [3] Hickok NJ, Shapiro IM, Chen AF. The impact of incorporating antimicrobials into implant surfaces. *J Dent Res.* 2018;97(1):14.
- [4] Liu R, Guo YL, Odusote G, Qu FL, Priestley RD. Core-shell Fe₃O₄ polydopamine nanoparticles serve multipurpose as drug carrier, catalyst support and carbon adsorbent. *ACS Appl Mater Interfaces.* 2013;5(18):9167.
- [5] Cheng W, Zeng XW, Chen HZ, Li ZM, Zeng WF, Mei L, Zhao YL. Versatile polydopamine platforms: synthesis and promising applications for surface modification and advanced nanomedicine. *ACS Nano.* 2019;13(8):8537.
- [6] Fu Y, Yang L, Zhang JH, Hu JF, Duan GG, Liu XH, Li YW, Gu ZP. Polydopamine antibacterial materials. *Mater Horizons.* 2021;8(6):1618.
- [7] Hu XY, Tian JH, Li C, Su H, Qin RR, Wang YF, Cao X, Yang P. Amyloid-like protein aggregates: a new class of bioinspired materials merging an interfacial anchor with antifouling. *Adv Mater.* 2020;32(23):2000128.
- [8] Jiang JH, Zhu LP, Zhu LJ, Zhang HT, Zhu BK, Xu YY. Antifouling and antimicrobial polymer membranes based on bioinspired polydopamine and strong hydrogen-bonded poly(*N*-vinyl pyrrolidone). *ACS Appl Mater Interfaces.* 2013;5(24):12895.
- [9] Cong Y, Xia T, Zou M, Li ZN, Peng B, Guo DZ, Deng ZW. Mussel-inspired polydopamine coating as a versatile platform for synthesizing polystyrene/ag nanocomposite particles with enhanced antibacterial activities. *J Mater Chem B.* 2014;2(22):3450.
- [10] Fu JW, Chen ZH, Wang MH, Liu SJ, Zhang JH, Zhang JN, Han RP, Xu Q. Adsorption of methylene blue by a high-efficiency adsorbent (polydopamine microspheres): kinetics, isotherm, thermodynamics and mechanism analysis. *Chem Eng J.* 2015;259:53.
- [11] Lee H, Dellatore SM, Miller MM, Messersmith PB. Mussel-inspired surface chemistry for multifunctional coatings. *Science.* 2007;318(5849):426.
- [12] Ye Q, Zhou F, Liu WM. Bioinspired catecholic chemistry for surface modification. *Chem Soc Rev.* 2011;40(7):4244.
- [13] Liu YL, Ai KL, Lu LH. Polydopamine and its derivative materials: synthesis and promising applications in energy, environmental, and biomedical fields. *Chem Rev.* 2014;114(9):5057.
- [14] Lyngé ME, Schattling P, Stadler B. Recent developments in poly(dopamine)-based coatings for biomedical applications. *Nanomedicine.* 2015;10(17):2725.
- [15] Batul R, Tamanna T, Khaliq A, Yu A. Recent progress in the biomedical applications of polydopamine nanostructures. *Biomater Sci.* 2017;5(7):1204.
- [16] Chen CT, Martin-Martinez FJ, Jung GS, Buehler MJ. Polydopamine and eumelanin molecular structures investigated with ab initio calculations. *Chem Sci.* 2017;8(2):1631.
- [17] Mrówczyński R, Markiewicz R, Liebscher J. Chemistry of polydopamine analogues. *Polym Int.* 2016;65(11):1288.
- [18] Batul R, Bhavne M, Mahon PJ, Yu A. Polydopamine nanosphere with in-situ loaded gentamicin and its antimicrobial activity. *Molecules.* 2020;25(9):2090.
- [19] Wu CJ, Zhang GX, Xia T, Li ZN, Zhao K, Deng ZW, Guo DZ, Peng B. Bioinspired synthesis of polydopamine/Ag nanocomposite particles with antibacterial activities. *Mater Sci Eng C.* 2015;55:155.
- [20] Ran HH, Cheng XT, Gao G, Sun W, Jiang YW, Zhang XD, Jia HR, Qiao Y, Wu FG. Colistin-loaded polydopamine nanospheres uniformly decorated with silver nanodots: a nanohybrid platform with improved antibacterial and antibiofilm performance. *ACS Appl Bio Mater.* 2020;3(4):2438.
- [21] Ma K, Dong P, Liang MJ, Yu SS, Chen YY, Wang F. Facile assembly of multifunctional antibacterial nanoplateform leveraging synergistic sensitization between silver nanostructure and vancomycin. *ACS Appl Mater Interfaces.* 2020;12(6):6955.
- [22] Shang B, Xu M, Zhi ZL, Xi YW, Wang YB, Peng B, Li P, Deng ZW. Synthesis of sandwich-structured silver@polydopamine@silver shells with enhanced antibacterial activities. *J Colloid Interface Sci.* 2020;558:47.
- [23] Wang Y, Su J, Li T, Ma PM, Bai HY, Xie Y, Chen MQ, Dong WF. A novel UV-shielding and transparent polymer film: when bioinspired dopamine-melanin hollow nanoparticles join polymers. *ACS Appl Mater Interfaces.* 2017;9(41):36281.
- [24] Li J, Tan L, Liu XM, Cui ZD, Yang XJ, Yeung KWK, Chu PK, Wu S. Balancing bacteria-osteoblast competition through selective physical puncture and biofunctionalization of ZnO/polydopamine/arginine-glycine-aspartic acid-cysteine nanorods. *ACS Nano.* 2017;11(11):11250.
- [25] Li LH, Yang L, Liao YB, Yu HC, Liang Z, Zhang B, Lan XR, Luo RF, Wang YB. Superhydrophilic versus normal polydopamine coating: a superior and robust platform for synergistic antibacterial and antithrombotic properties. *Chem Eng J.* 2020;402:126196.
- [26] Xu YW, Ji YL, Ma JH. Hydrophobic and hydrophilic effects in a mussel-inspired citrate-based adhesive. *Langmuir.* 2021;37(1):311.
- [27] Wonderly WR, Cristiani TR, Cunha KC, Degen GD, Shea JE, Waite JH. Dueling backbones: comparing peptoid and peptide analogues of a mussel adhesive protein. *Macromolecules.* 2020;53(16):6767.
- [28] El Yakhlifi S, Alfieri M-L, Arntz Y, Eredia M, Ciesielski A, Samorì P, d'Ischia M, Ball V. Oxidant-dependent antioxidant activity of polydopamine films: The chemistry-morphology interplay. *Colloids Surf Physicochem Eng Aspects.* 2021;614:126134.
- [29] Lee H, Scherer NF, Messersmith PB. Single-molecule mechanics of mussel adhesion. *Proc Natl Acad Sci U S A.* 2006;103(35):12999.
- [30] Priemel T, Palia R, Babych M, Thibodeaux CJ, Bourgault S, Harrington MJ. Compartmentalized processing of catechols during mussel byssus fabrication determines the destiny of DOPA. *Proc Natl Acad Sci U S A.* 2020;117(14):7613.
- [31] Wang Z, Zou Y, Li YW, Cheng YY. Metal-containing polydopamine nanomaterials: catalysis, energy, and theranostics. *Small.* 2020;16(18):1907042.
- [32] Xi ZY, Xu YY, Zhu LP, Wang Y, Zhu BK. A facile method of surface modification for hydrophobic polymer membranes based on the adhesive behavior of poly(DOPA) and poly(dopamine). *J Membrane Sci.* 2009;327(1–2):244.
- [33] Ryu JH, Messersmith PB, Lee H. Polydopamine surface chemistry: a decade of discovery. *ACS Appl Mater Interfaces.* 2018;10(9):7523.
- [34] Guo XJ, Cao B, Wang CY, Lu SY, Hu XL. In vivo photothermal inhibition of methicillin-resistant staphylococcus aureus infection by in situ templated formulation of pathogen-targeting phototheranostics. *Nanoscale.* 2020;12(14):7651.
- [35] Au KM, Lu Z, Matcher SJ, Armes SP. Polypyrrole nanoparticles: a potential optical coherence tomography contrast agent for cancer imaging. *Adv Mater.* 2011;23(48):5792.
- [36] Luo P, Wang SN, Zhao TT, Li Y. Surface characteristics, corrosion behavior, and antibacterial property of Ag-implanted nit alloy. *Rare Met.* 2013;32(2):113.
- [37] Samanta A, Podder S, Kumarasamy M, Ghosh CK, Lahiri D, Roy P, Bhattacharjee S, Ghosh J, Mukhopadhyay AK. Au nanoparticle-decorated aragonite microdumbbells for enhanced

- antibacterial and anticancer activities. *Mater Sci Eng C*. 2019; 103:109734.
- [38] Li Y, Tian Y, Zheng WS, Feng Y, Huang R, Shao JX, Tang RB, Wang P, Jia YX, Zhang JJ, Zheng WF, Yang G, Jiang XY. Composites of bacterial cellulose and small molecule-decorated gold nanoparticles for treating Gram-negative bacteria-infected wounds. *Small*. 2017;13(27):1700130.
- [39] Rajan A, Vilas V, Philip D. Studies on catalytic, antioxidant, antibacterial and anticancer activities of biogenic gold nanoparticles. *J Mol Liq*. 2015;212:331.
- [40] Kim JH, Joshi MK, Lee J, Park CH, Kim CS. Polydopamine-assisted immobilization of hierarchical zinc oxide nanostructures on electrospun nanofibrous membrane for photocatalysis and antimicrobial activity. *J Colloid Interface Sci*. 2018;513:566.
- [41] Islam MS, Akter N, Rahman MM, Shi C, Islam MT, Zeng H, Azam MS. Mussel-inspired immobilization of silver nanoparticles toward antimicrobial cellulose paper. *ACS Sustain Chem Eng*. 2018;6(7):9178.
- [42] Wu HQ, Liu YJ, Huang J, Mao L, Chen JH, Li M. Preparation and characterization of antifouling and antibacterial polysulfone ultrafiltration membranes incorporated with a silver-polydopamine nanohybrid. *J Appl Polym Sci*. 2018;135(27):46430.
- [43] Coelho D, Sampaio A, Silva C, Felgueiras HP, Amorim MTP, Zille A. Antibacterial electrospun poly(vinyl alcohol)/enzymatic synthesized poly(catechol) nanofibrous midlayer membrane for ultrafiltration. *ACS Appl Mater Interfaces*. 2017;9(38):33107.
- [44] Zhang QM, Wang YL, Zhang WK, Hickey ME, Lin ZS, Tu Q, Wang JY. In situ assembly of well-dispersed Ag nanoparticles on the surface of polylactic acid-Au@polydopamine nanofibers for antimicrobial applications. *Colloids Surf B*. 2019;184:110506.
- [45] Zhou ZW, Liu R. Fe₃O₄@polydopamine and derived Fe₃O₄@carbon core-shell nanoparticles: comparison in adsorption for cationic and anionic dyes. *Colloid Surf A*. 2017;522:260.
- [46] Guo LQ, Liu Q, Li GL, Shi JB, Liu JY, Wang T, Jiang GB. A mussel-inspired polydopamine coating as a versatile platform for the in situ synthesis of graphene-based nanocomposites. *Nanoscale*. 2012;4(19):5864.
- [47] Ma R, Yang P, Ma Y, Bian F. Facile synthesis of magnetic hierarchical core-shell structured Fe₃O₄@PDA-Pd@MOF nanocomposites: highly integrated multifunctional catalysts. *ChemCatChem*. 2018;10(6):1446.
- [48] Zhao FJ, Lei B, Li X, Mo YF, Wang RX, Chen DF, Chen XF. Promoting in vivo early angiogenesis with sub-micrometer strontium-contained bioactive microspheres through modulating macrophage phenotypes. *Biomaterials*. 2018;178:36.
- [49] Miguez-Pacheco V, Hench LL, Boccaccini AR. Bioactive glasses beyond bone and teeth: emerging applications in contact with soft tissues. *Acta Biomater*. 2015;13:1.
- [50] Lei B, Guo BL, Rambhia KJ, Ma PX. Hybrid polymer biomaterials for bone tissue regeneration. *Front Med*. 2019;13(2):189.
- [51] Han L, Liu KZ, Wang MH, Wang KF, Fang LM, Chen HT, Zhou J, Lu X. Mussel-inspired adhesive and conductive hydrogel with long-lasting moisture and extreme temperature tolerance. *Adv Funct Mater*. 2018;28(3):1704195.
- [52] Zhou L, Xi YW, Xue YM, Wang M, Liu YL, Guo Y, Lei B. Injectable self-healing antibacterial bioactive polypeptide-based hybrid nanosystems for efficiently treating multidrug resistant infection, skin-tumor therapy, and enhancing wound healing. *Adv Funct Mater*. 2019;29(22):1806883.
- [53] Park JK, Kim YJ, Yeom J, Jeon JH, Yi GC, Je JH, Hahn SK. The topographic effect of zinc oxide nanoflowers on osteoblast growth and osseointegration. *Adv Mater*. 2010;22(43):4857.
- [54] Wang ZL. ZnO nanowire and nanobelt platform for nanotechnology. *Mater Sci Eng R Rep*. 2009;64(3-4):33.
- [55] Zaveri TD, Dolgova NV, Chu BH, Lee J, Wong J, Lele TP, Ren F, Keselowsky BG. Contributions of surface topography and cytotoxicity to the macrophage response to zinc oxide nanorods. *Biomaterials*. 2010;31(11):2999.
- [56] Wang TT, Liu XM, Zhu YZ, Cui ZD, Yang XJ, Pan H, Yeung KWK, Wu SL. Metal ion coordination polymer-capped pH-triggered drug release system on titania nanotubes for enhancing self-antibacterial capability of Ti implants. *ACS Biomater Sci Eng*. 2017;3(5):816.
- [57] Huang L, Liu MY, Huang HY, Wen YQ, Zhang XY, Wei Y. Recent advances and progress on melanin-like materials and their biomedical applications. *Biomacromol*. 2018;19(6):1858.
- [58] Xiang YM, Mao CY, Liu XM, Cui ZD, Jing DD, Yang XJ, Liang YQ, Li ZY, Zhu SL, Zheng YF, Yeung KWK, Zheng D, Wang XB, Wu SL. Rapid and superior bacteria killing of carbon quantum dots/ZnO decorated injectable folic acid-conjugated pda hydrogel through dual-light triggered ros and membrane permeability. *Small*. 2019;15(22):1900322.
- [59] Madhurakkat Perikamana SK, Lee J, Lee YB, Shin YM, Lee EJ, Mikos AG, Shin H. Materials from mussel-inspired chemistry for cell and tissue engineering applications. *Biomacromol*. 2015; 16(9):2541.
- [60] Lee BS, Lin YC, Hsu WC, Hou CH, Shyue JJ, Hsiao SY, Wu PJ, Lee YT, Luo SC. Engineering antifouling and antibacterial stainless steel for orthodontic appliances through layer-by-layer deposition of nanocomposite coatings. *ACS Appl Bio Mater*. 2019;3(1):486.
- [61] Bauer S, Schmuki P, von der Mark K, Park J. Engineering biocompatible implant surfaces. *Prog Mater Sci*. 2013;58(3): 261.
- [62] Zhang S, Liang XJ, Gadd GM, Zhao Q. Advanced titanium dioxide-polytetrafluorethylene (TiO₂-PTFE) nanocomposite coatings on stainless steel surfaces with antibacterial and anti-corrosion properties. *Appl Surf Sci*. 2019;490:231.
- [63] Schoon J, Hesse B, Rakow A, Ort MJ, Lagrange A, Jacobi D, Winter A, Katrin H, Reinke S, Cotte M, Tucoulou R, Marx U, Perka C, Duda GN, Geissler S. Metal-specific biomaterial accumulation in human peri-implant bone and bone marrow. *Adv Sci*. 2020;7(20):2000412.
- [64] Huang L, Su K, Zheng YF, Yeung KWK, Liu XM. Construction of TiO₂/silane nanofilm on AZ31 magnesium alloy for controlled degradability and enhanced biocompatibility. *Rare Met*. 2019;38(6):588.
- [65] Huang YJ, Ding XK, Qi YK, Yu B, Xu FJ. Reduction-responsive multifunctional hyperbranched polyaminoglycosides with excellent antibacterial activity, biocompatibility and gene transfection capability. *Biomaterials*. 2016;106:134.
- [66] Huang YS, Huang HH. Effects of clinical dental implant abutment materials and their surface characteristics on initial bacterial adhesion. *Rare Met*. 2019;38(6):512.
- [67] Zeng Q, Zhu YW, Yu BR, Sun YJ, Ding XK, Xu C, Wu YW, Tang ZH, Xu FJ. Antimicrobial and antifouling polymeric agents for surface functionalization of medical implants. *Biomacromol*. 2018;19(7):2805.
- [68] Lee JS, Lee SJ, Yang SB, Lee D, Nah H, Heo DN, Moon HJ, Hwang YS, Reis RL, Moon JH, Kwon IK. Facile preparation of mussel-inspired antibiotic-decorated titanium surfaces with enhanced antibacterial activity for implant applications. *Appl Surf Sci*. 2019;496:143675.
- [69] Wang C, Zhao W, Cao B, Wang Z, Zhou Q, Lu S, Lu L, Zhan M, Hu X. Biofilm-responsive polymeric nanoparticles with self-adaptive deep penetration for in vivo photothermal treatment of implant infection. *Chem Mater*. 2020;32(18): 7725.
- [70] Cao B, Lyu XM, Wang YC, Lu SY, Xing D, Hu XL. Rational collaborative ablation of bacterial biofilms ignited by physical



cavitation and concurrent deep antibiotic release. *Biomaterials*. 2020;262:120341.

- [71] Yu MM, Ding XJ, Zhu YW, Wu SM, Ding XK, Li Y, Yu BR, Xu FJ. Facile surface multi-functionalization of biomedical catheters with dual-microcrystalline broad-spectrum antibacterial drugs and antifouling poly(ethylene glycol) for effective inhibition of bacterial infections. *ACS Appl Bio Mater*. 2019; 2(3):1348.
- [72] Peng LY, Chang L, Liu X, Lin JX, Liu HL, Han B, Wang ST. Antibacterial property of a polyethylene glycol-grafted dental material. *ACS Appl Mater Interfaces*. 2017;9(21):17688.
- [73] Xiao FF, Cao B, Wang CY, Guo XJ, Li MG, Xing D, Hu XL. Retraction of “pathogen-specific polymeric antimicrobials with significant membrane disruption and enhanced photodynamic damage to inhibit highly opportunistic bacteria.” *ACS Nano*. 2020;14(5):6357.
- [74] Ho DH, Cheon S, Hong P, Park JH, Suk JW, Kim DH, Han JT, Cho JH. Multifunctional smart textiles with blow-spun non-woven fabrics. *Adv Funct Mater*. 2019;29(24):1900025.
- [75] Zhu YW, Xu C, Zhang N, Ding XK, Yu BR, Xu FJ. Polycationic synergistic antibacterial agents with multiple functional components for efficient anti-infective therapy. *Adv Funct Mater*. 2018;28(14):1706709.



Ju-Lin Wang received her Ph.D. degree from Beijing University of Chemical Technology in 2004 and then worked as a professor at Beijing University of Chemical Technology up to now. Her main research interests focus on cultural heritage conservation and material failure mechanism. In China, she is an academic leader in the field of cultural relics preservation.



corresponding author.

Bing-Ran Yu is a professor at Beijing University of Chemical Technology. He obtained his Ph.D. degree in inorganic chemistry from Lanzhou University in 2013 and then joined Beijing University of Chemical Technology. Dr. Yu has contributed significantly to the field of design, construction, and application of drug/gene delivery vectors and novel antibacterial polymers. He has published more than 30 articles in international journals as the